12-15-2017 2:00 PM

A performance based design approach for tall buildings under wind loading

Fouad Y. Elezaby
The University of Western Ontario

Supervisor
El Damatty, A.
The University of Western Ontario

Graduate Program in Civil and Environmental Engineering
A thesis submitted in partial fulfillment of the requirements for the degree in Master of Science

ABSTRACT

The wind design of buildings is typically based on strength provisions under ultimate loads. This is unlike the ductility-based approach used in seismic design, which allows inelastic actions to take place in the structure under extreme seismic events. This research investigates the application of a similar concept in wind engineering. In seismic design, the elastic forces resulting from an extreme event of high return period are reduced by a load reduction factor. A load reduction factor is chosen by the designer and accordingly a certain ductility capacity needs to be achieved in the structure. Two reasons have triggered the investigation of this ductility-based concept under wind loads. First, there is a trend in the design codes to increase the return period used in wind design approaching the large return period used in seismic design. Second, the structure always possesses a certain level of ductility that the wind design does not benefit from. The load reduction factor that could be applied in wind design might not be as high as its counterpart in seismic design, and it should be applied only on the resonant component of the wind loading. Many technical issues arise when applying a ductility-based approach under wind loads. The use of reduced design loads will lead to the design of a more flexible structure with larger natural periods. While this might be beneficial for seismic response, it is not necessarily the case for the wind response, where increasing the flexibility is expected to increase the fluctuating response. This particular issue is examined by considering a case study of a sixty five-story high-rise building previously tested at the Wind Tunnel Laboratory at the University of Western Ontario using a pressure model. A three-dimensional finite element model is developed for the building. The wind pressures from the tested rigid model are applied to the finite element model and a time history dynamic analysis is conducted. The time history variation of the straining actions on various structure elements of the

building are evaluated and decomposed into mean, background and fluctuating components. A reduction factor is applied to the fluctuating components and a modified time history response of the straining actions is calculated. The building components are redesigned under this set of reduced straining actions and its fundamental period is then evaluated. A new set of loads is calculated based on the modified period and is compared to the set of loads associated with the original structure.

This is followed by non-linear static pushover analysis conducted individually on each shear wall module after redesigning these walls. Displacement-controlled pushover analysis is carried out to assess the ductility demand of shear walls with reduced cross sections to justify the application of the load reduction factor “R”. Furthermore, a parametric study is conduced to evaluate the effect of ductility level on target performance level reached in each shear wall.

Keywords

Performance-based design, Wind tunnel test, Dynamic Time-History analysis, High-rise buildings, Non-linear analysis, Static-pushover analysis, Shear wall ductility.

To my parents ***Yehia Elezaby*** and ***Suzan Elezaby***

To my brothers ***Kamal*** and ***Ibrahim*** and my sister ***Sarah***

For their support, caring, encouragement and sharing these years of hard work

To my supervisor, ***Dr. Ashraf A. El Damatty***

For his guidance and support, as well as sharing his experience during these years

ACKNOWLEDGEMENTS

First of all, I would like to thank Allah (the almighty) for all his blessings and mercy, and give us all the support and inspiration to complete this work. If it weren't for Allah's presence, I wouldn't have had the patience and persistence to reach this milestone in my life.

With boundless love and appreciation, I would like to express with these simple yet sincere word my thanks and gratitude to all those who helped me through the past years, to bring this study into reality which would have never been possible without their help.

I would like to thank my supervisor Dr. Ashraf A. El Damatty for his continuous help and support throughout my masters. I really owe him all the knowledge and skills he has provided me with. I am grateful for all the encouragement and the long hours he has spent with me to provide me with his valuable experience and learning new approaches on how to deal with complicated research problems.

I would like to acknowledge the collaboration of Dar Group Consultants – Shair and Partners for providing us with the structural drawings for our case study. I would also like to thank the Boundary Layer Wind Tunnel (BLWT) facility at Western University for providing us with the wind tunnel data and guidance on post-processing of these data.

From the deep of my heart, I would like to thank my lovely family for their patience and continuous support during my journey here despite of the long distances. Words would fall short to describe my admiration and thanks to all what you have given me; my lovely and caring mother, thank you for always being there for me and for your everyday prayers; my father, thanks for always giving me advice as a parent and as a field professional. All my siblings, thanks for always showing care

and support. To my beloved family, I owe you everything I have achieved so far, and I wish I could always make you proud.

I am extremely thankful for the help I received from Dr. Ayman El Ansary and Dr. Ahmed Elshaer who really took long hours of their time to support and guide me through my Masters program. The support of all my friends and colleagues at Western is truly appreciated. Many thanks must go to (A. Musa, A. Ibrahim, M. Aboutabikh, A. El Ansary, A. AbdelKader, A. Shehata, I. Ibrahim, M. Hamada, A. Elawady, A. Fayez, H. Aboshosha, M. Elsawy, S. Elrouby, M. Ajan Elhadid, A. Adawi, M. Mansour, M. Kasem, M, Askar, O. Elhawary). I want also to thank all my international friends I met at Western from everywhere around the world, you all really enriched my knowledge and made my experience at Western an unforgettable one.

TABLE OF CONTENTS

LIST OF TABLES

LIST OF FIGURES

CHAPTER 1

INTRODUCTION

1.1 General

Buildings subjected to wind forces are designed using elastic analysis and equivalent static lateral loads prescribed in building codes. Recent trends and modern architectural requirements have pushed towards developing increasingly taller and irregularly- shaped complex buildings, leading to structures that are potentially more susceptible to wind excitations. As buildings become taller and more slender, they become more vulnerable to wind excitations than to earthquake effects. However, significant benefits can be obtained with the adoption of a performance-based technique, where member inelastic behavior and dynamic effects of the natural hazard are explicitly considered. Such strategies have been successfully adopted in seismic engineering.

Performance-based design is an attempt to design buildings with predictable loading-induced performance, rather than being based on empirical code specifications. The earthquakes and extreme winds are the two major loading conditions experienced through the lifetime of buildings. While the performance-based seismic design (PBSD) is becoming well known in professional practice for the design of buildings under seismic loading, the wind-induced performance-based design (WPBD) is also emerging as a promising design methodology to improve the current practice in the tall building design against wind.

Performance-based wind engineering has been identified as a national research priority (CTBUH 2014). Nonlinear analysis has been used to determine the structural reliability of tall concrete buildings (Hart and Jain 2014), but general application of nonlinear analysis to performance-based

wind analysis is still undeveloped. One motivation for a nonlinear wind analysis is that prescribed code method in wind design may be overly conservative. Member stresses are limited to the linear elastic range for strength-level events. Another motivation for a nonlinear analysis is to determine collapse capacity of buildings. An additional motivation that triggered the investigation of this subject is the fact that there has been a trend recently in current codes to increase the return period employed in design wind speed approaching the large return period used in seismic design. Furthermore, architetecutral requirements are becoming more complicated, which can encourage structural design to aim at reducing structural members cross sections.

Performance-based design (PBD) is rapidly becoming the benchmark approach for the design of structures to resist lateral loads. In the design of building systems against earthquakes, the principles of PBD have been widely adopted as a means for achieving earthquake resilient designs. Many of the prescriptions contained in international building codes and standards that govern seismic design can be linked back to the principles of PBD (e.g. Eurocode 8 and the ASCE 7-10) and also capacity design procedures as defined by NBCC 2010 . As an approach, PBD focuses on the definition of a set of performance objectives that must be satisfied by the building system under investigation.

A key challenge in performance-based wind engineering is how to apply nonlinear analysis to predict inelastic building behavior and the risk of collapse for wind loads. The difficulty of a nonlinear analysis for wind, as opposed to seismic loads, mainly arises from inherent differences in the hazards. Wind loads are generated by wind pressures applied to the building envelope, whereas seismic loads are inertial forces generated by ground movement. The characteristics of

wind pressure depend primarily on the shape of the building and the terrain exposure. Wind loads also depend on the type of windstorm (e.g. hurricane, extra-tropical cyclone, downburst, and tornado). This differs from seismic load characteristics, which depend largely on the mass of the building and the tectonic environment, fault mechanism, and epicenteral distance.

When existing buildings are subject to alterations in later design stages such as a change in the cladding system, owners may need to evaluate the adequacy of the lateral load resisting system. For designs governed by wind loads, the standard approach is to evaluate building performance under current codes. This involves an elastic analysis of the building subjected to code-prescribed or wind tunnel equivalent static wind loads, followed by an evaluation of the building behavior at service and strength limit states. For structural members not satisfying code limits, rehabilitation measures are prescribed. An alternate approach is to consider a performance-based evaluation, similar to the current state of the art in building designs governed by seismic loads (ASCE 2003; ASCE 2007).

The merits of a performance-based approach include a more accurate analysis of building response with explicit consideration of nonlinear behavior. In traditional building design procedures, cracking factors are used to represent nonlinear behavior, which is less accurate. Furthermore, a performance-based approach allows for an explicit evaluation of the building's performance at a particular hazard level, which is generally not assessed as part of the traditional prescribed code method.

Performance-based design (PBD) represents the most advanced and rational way of addressing the societal need for safety when designing civil structures. In a traditional code-based design process,

design professionals ensure the satisfaction of prescriptive criteria which, even though established based on a certain level of expected performance, do not guarantee the correct evaluation and understanding of the actual reliability achieved (Ellingwood 2001, FEMA 2012a).

In the case of PBD, on the other hand, the performance of the structure is directly linked to the probability of experiencing different types of losses, which can result from natural or man-made hazards over the entire lifetime of the structure.

1.2 Literature

To date, there has been several proposed frameworks for performance-based wind design according to Van de Lindt (2009), Ciampoli et al. (2011), Griffis (2013a) and Griffis et al (2013b). Bakhshi and Nikhbakht (2011) performed nonlinear analyses of 20 to 40- story steel frame buildings in a parametric study comparing earthquake and wind loads, at strength-level hazard intensity. Muthukumar et al. (2012) performed a nonlinear dynamic analysis of an existing 22-story reinforced-concrete shear wall building up to strength-level wind intensities, but did not attempt to evaluate collapse.

Gani and Legeron (2012) predicted the nonlinear response of single-degree-of-freedom (SDOF) models using a spectral stochastic method, exhibiting simple behavior (elastic, perfectly-plastic, and bilinear with strain hardening). However, this approach required use of an equivalent elastic system.

Huang et al. (2015) presented an integrated computational design optimization method for the performance-based design of high-rise buildings subjected to different levels of wind excitation.

They proposed a performance-based design defining different performance objectives associated with multiple levels of wind hazards. In this study, nonlinear static pushover analysis was conducted to evaluate inelastic drifts resulting from wind events with very high return periods. The augmented optimality criteria method was used to formulate and solve the optimal performance-based design problem considering inelastic deformation. The proposed framework was applied on a practical 40-story residential building.

Muthukumar et al. (2013) presented an evaluation of the Main Wind Force Resisting System (MWFRS) of an existing building, whose façade was proposed to be replaced with a new curtain wall system. The building did not meet the strength limit state prescribed under current codes. Therefore, a performance-based evaluation approach was utilized as per the framework outlined in Griffis et al. (2012). Structural testing, non-destructive evaluations and visual assessments were conducted to determine the condition of the existing structure and develop as-built data for the performance-based evaluation. Inelastic behavior of the shear walls was explicitly modeled. Wind loads were obtained from wind tunnel testing performed at Rowan, Williams, Davies, and Irwin, Inc. (RWDI). Building target performance levels were established at both the service and strength limit states. Nonlinear analyses were then conducted to evaluate building performance at the identified target levels.

Judd and Charney (2015) performed nonlinear dynamic analyses to examine inelastic behavior and collapse risk for a 10-story SDOF model for a steel building based on a characteristic main wind-force resisting system (MWFRS) in the longitudinal direction. The study investigated the inelastic behaviour and risk of collapse of SDOF models. The study was also used to investigate if the application of a load factor “R” similar to that employed in seismic design would result in

an economic design. For the specific building studied, ductility demand was effective in increasing the collapse safety and reducing risk of collapse. It was concluded that by providing a limited level of ductility for the moment frame system, it was justified to use a load reduction factor of R = 1.25.

Spence and Kareem (2014) developed a framework for the probabilistic performance-based assessment of large-scale uncertain linear systems driven by experimentally stochastic wind loads. The study was done on a 45 story steel building with an offset core. The members under study were box section columns. Several other probabilistic performance-based design approaches were proposed by Paulotto et al. (2004), Bashor and Kareem (2007), Augusti and Ciampoli (2008), and Ciampoli et al. (2011).

Spence et al. (2015) presented a first attempt to define an appropriate framework to allow the principles of performance-based design to be employed during the design of building systems to resist severe wind events. Focus was placed on highlighting the necessary steps to reach such a goal, which include the definition of site-specific wind hazard models, of suitable fragility functions as well as of consequence functions that rationally assess damage and losses.

Ciampoli et al. (2011) first extended the approach proposed by the Pacific Earthquake Engineering Research Center (PEER) for Performance-Based Earthquake Engineering is extended to the case of Performance-Based Wind Engineering. The framework was applied on a long span suspension bridge, and the assessment of collapse and out-of-service risks were illustrated.

1.3 Research Gaps

The previously mentioned studies focused on proposing probabilistic approaches for performance-based wind engineering. Inherent ductility in concrete members has not been explicitly considered before in a defined framework. Wind design has not yet benefited from such property of reinforced concrete, as it is the case in seismic design. Current codes only use equivalent static wind loads, which can be overly conservative. Furthermore, there has been a trend recently in current codes to increase the design wind event return period, but on the other hand, it should be guaranteed that members possess enough ductility to experience inelastic actions without major loss in strength. As such, it is important to define a framework for a performance-based technique, and define target performance levels as limits define in ASCE/SEI 41-13 to be used as a guide in assessment.

Based on the addressed gaps in literature, the current thesis focuses on proposing a framework for a performance based design for buildings subjected to wind loads, and application of this framework on a high-rise building, as well as assessing the inelastic actions experienced by concrete shear walls.

1.4 Thesis Objectives

The main objectives of this thesis are summarized as follows:

1- Develop a framework for performance-based design for buildings subjected to extreme wind loads.
2- Investigate the applicability of ductility-based approach adopted in building codes for seismic design (NBCC 2010) on wind design.
3- Assess the inelastic behaviour of concrete shear walls under wind loads.

1.5 Thesis Organization

The thesis has been prepared in a monograph format. In chapter 1, a review of the literature related to the applications and importance of implementing a performance-based procedure for high-rise building subjected to wind is presented. This is followed by addressing the gaps in the literature and outlining the objectives of the thesis. In chapter 2, a finite-element numerical model is developed for a high-rise building, and wind loads from wind tunnel testing are applied to evaluate the full dynamic and quasi-static responses of the building. In chapter 3, non-linear static pushover analysis is conducted on concrete shear walls to assess ductility demand and determine target performance levels reached for each shear wall.

1.5.1 Preliminary Investigation to Assess the Application of Ductility – Based Approach for High-Rise Buildings subjected to extreme Wind Loads.

In this chapter, a 3D finite element model is constructed for a 65 storey building using ETABS software. The building main lateral load resisting system is concrete shear walls. Wind loads are taken from wind tunnel pressure test results. Testing was conducted at the Boundary Layer wind Tunnel (BLWT) facility at the University of Western Ontario. Dynamic time history analysis is conducted to calculate full dynamic responses of the building (base shear, base moments, and displacements). This is followed by Quasi-static analysis to calculate the Mean and Background responses. Furthermore, wind response is decomposed into Mean, Background and Resonant component. Load reduction factor "R" similar to that applied in seismic design is applied on wind resonant component, and accordingly, concrete shear walls are redesigned. Building dynamic characteristics are compared before and after reduction of shear walls. The same procedure is implemented using different reduction factors.

1.5.2 Non-linear Static Analysis for Ductility- Based Designed Reinforced Concrete Shear Walls Subjected to Extreme Wind Loads.

In this chapter, a numerical 2-D finite element model is developed for concrete shear walls individually to conduct static-pushover analysis on reduced cross-sections based on the reduction procedure described in chapter 2. Load pattern for pushover analysis is taken as the shear force diagram applied on shear walls resulting from elastic analysis conducted in chapter 2. Displacement-controlled pushover analysis is carried out and ductility demand (μ) of each shear wall module is evaluated.

Furthermore, target performance levels reached for each shear wall is evaluated and compared with limits of acceptance criteria set by current building codes (ASCE/SEI 41-13). The same analysis is repeated using different levels of ductility for shear walls, which can be achieved through different detailing provisions as mentioned in current codes (NBCC 2010).

CHAPTER 2

PRELIMENARY INVESTATION TO ASSESS THE APPLICATION OF DUCTLITY- BASED APPROACH FOR HIGH-RISE BUILDINGS SUBJECTED TO EXTREME WIND LOADS

2.1 Introduction

Buildings subjected to wind loads are traditionally designed considering only the elastic range of members and using equivalent static loads and prescribed code methods. It has not been considered before to take inherent ductility in structural members into consideration. Therefore, the implementation of a performance-based design for structures under wind loads would be beneficial, where inelastic behavior of members are considered.

In seismic design, controlled inelastic actions are permitted in lateral load resisting system members but under condition that these members possess a certain level of ductility. One motivation for adopting a ductility-based design is that there has been a trend in design codes lately to increase the return period as per ASCE 7-10. Another motivation is that wind design has not benefited so far from inherent ductility in members, which can affect the design of structural members and may result in savings in the structural costs in high-rise buildings. This chapter investigates application of performance-based approach on a high-rise building under extreme wind loads. A framework for performance-based design is proposed. First, a 3D finite element model for the building is developed. Then the applicability of the proposed framework is tested on a 65 storey high-rise building. Through a series of steps: 1) conducting dynamic time-history analysis to evaluate building responses (base shear, bending moments, and displacements). 2) Separating wind response into mean and background component and resonant component alone.

3) Reducing wind resonant component by "R" factor. 4) Comparing the dynamic characteristic and modes shapes of the structure before and after cross section reduction.

2.2 Flowchart for the proposed Performance - Based Design framework

In this section, a proposed framework for performance – based design for high-rise buildings subjected to wind forces is presented. First, wind tunnel data is taken and processed to evaluate story forces that are applied on a 3D finite element model. Time history dynamic analysis is conducted to evaluate total response of the building (base shear $V_T(t)$, base moment $M_T(t)$ and displacements $\Delta_T(t)$). Second, the response fluctuating part is decomposed into background and resonant component by conducting Quasi-Static analysis and evaluating Mean + Background component then subtracting this part from the total response to get the resonant part. Then, the resonant part is to be reduced by an R factor as adopted in seismic design and a new set of loads are applied to the lateral load resisting system members and accordingly, members are redesigned under the reduced straining actions. Furthermore, the dynamic characteristics of the structure with the reduced cross sections are checked and compared with the initial design in terms of fundamental period and total base shear. The scope of this chapter is concerned up to this step in the flowchart. The next step is to check if the structure possesses enough ductility, and assess the inelastic actions of the reduced cross sections. This issue is addressed in chapter 3. **Fig. 2- 1** shows the proposed framework for the performance based- design procedure. It should be noted that this study is preliminary in its nature and only limited to the case study presented in this thesis.

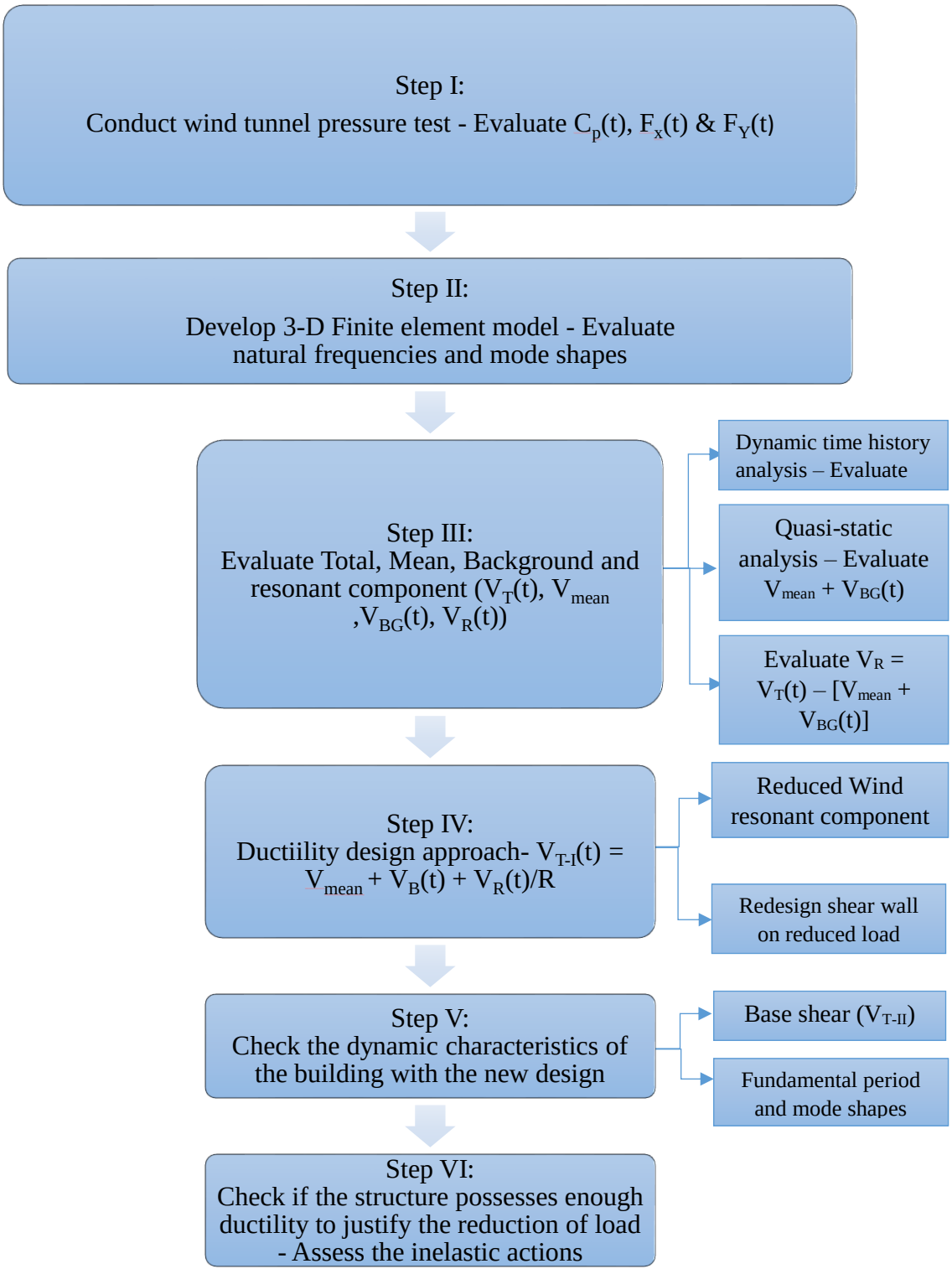

Fig. 2- 1: Proposed framework for Performance-based design

2.3 Step I: Wind tunnel testing

2.3.1 Building description

The study is done on a commercial building that consists of 65 stories with a total height of 232 m and overall plan dimensions of approximately 50 m X 70 m. The structure's main lateral load resisting system is concrete shear walls. The structural system for the typical story is flat slab with spans ranging between 7m and 9m. **Fig. 2- 2** shows the layout for the whole site.

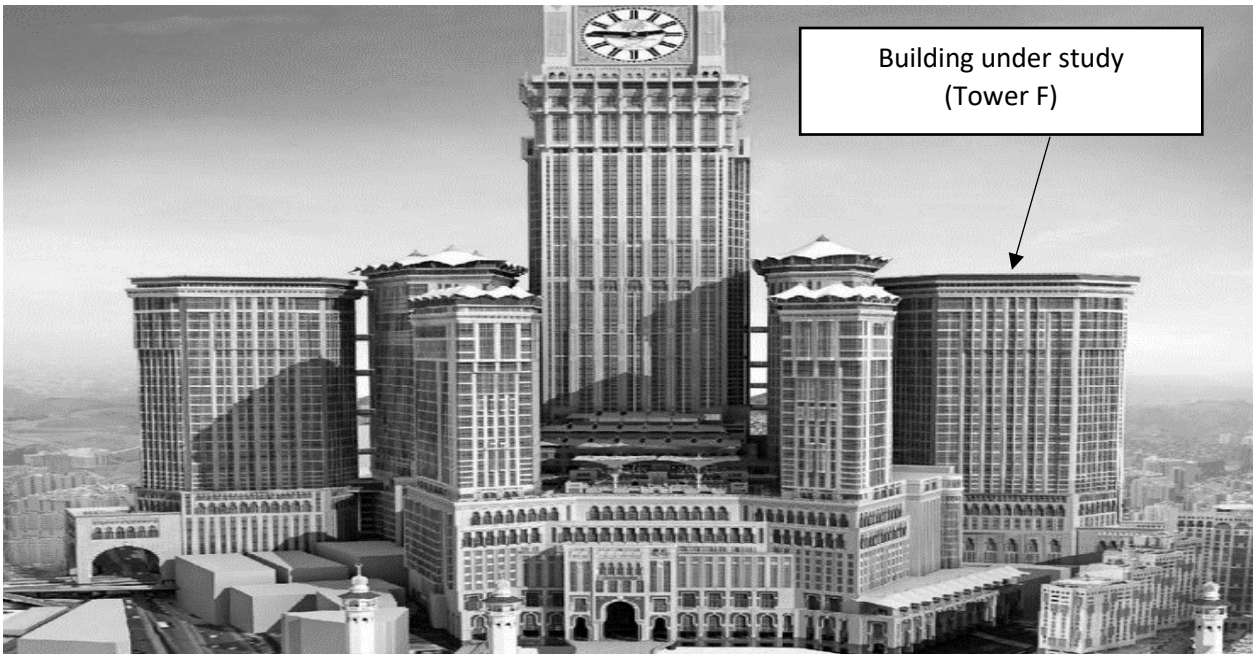

Fig. 2- 2: Layout for the project site (Source: Wikipedia: https://en.wikipedia.org/wiki/Abraj_Al_Bait)

The building under study is Tower F as shown in **Fig. 2- 3** in the project layout. The building is functioning as a hotel. Initially the building was designed for strength as per building code ACI 318-95, which was as a baseline for comparison of the dynamic characteristics of the structure after applying the reduction procedure on wind resonant component described in this chapter.

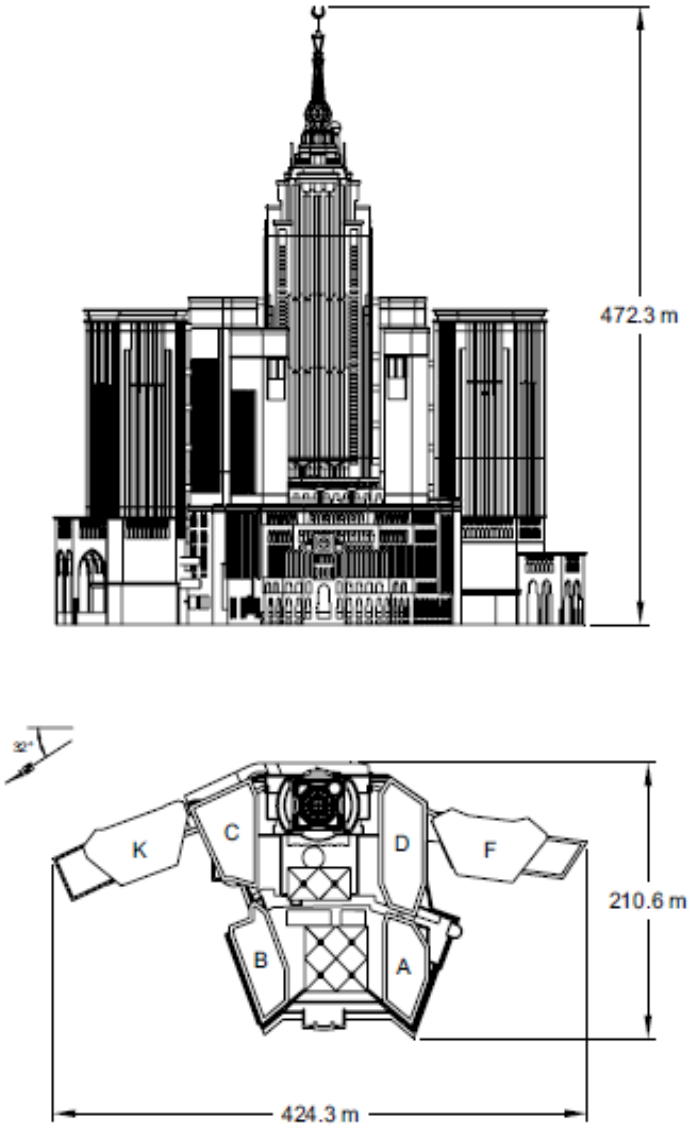

Fig. 2- 3: Elevation and plan views for the layout (Boundary Layer Wind Tunnel report, 2008)

2.3.2 Wind data at building location

The predicted 50-year and 100-year return period hourly mean wind speeds at gradient level (300 m height) at the location of the building are 35 m/s and 38 m/s respectively as shown in **Fig. 2- 4**. The most critical wind directions are those coming from West and North-West directions as shown in **Fig. 2- 5** in the building location wind rose.

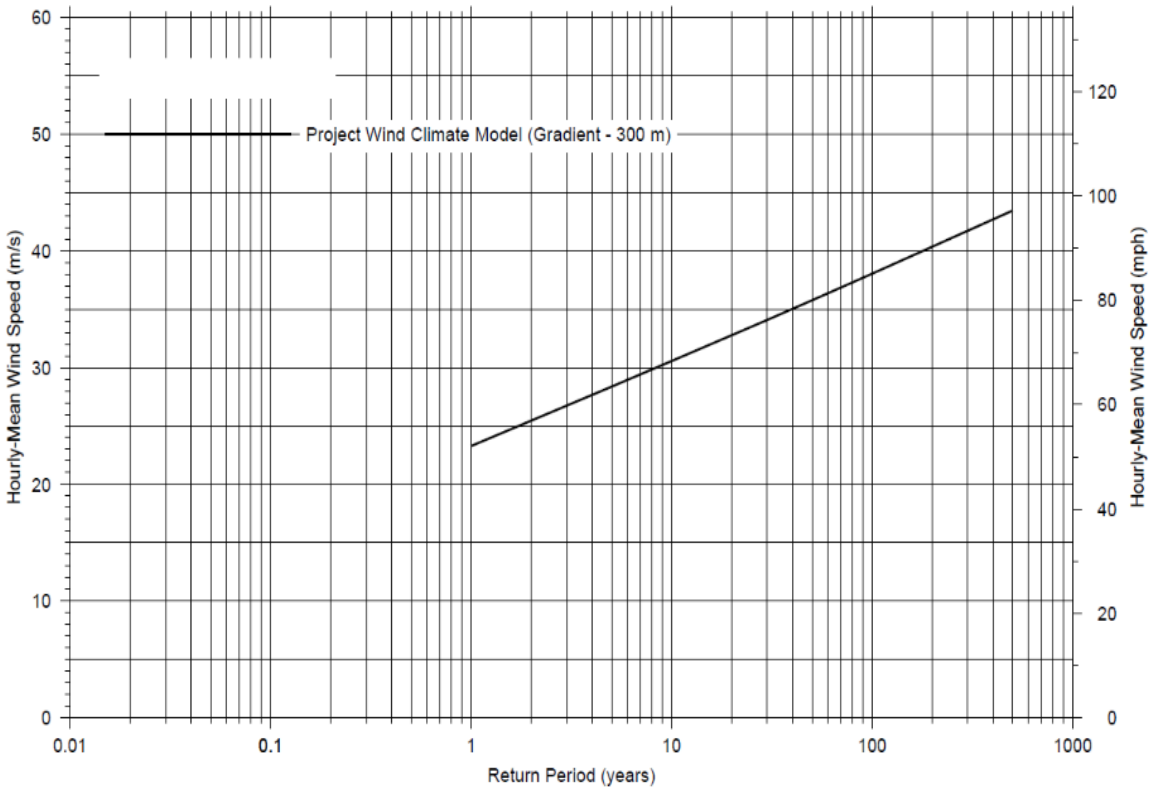

Fig. 2- 4: Hourly- Mean wind speeds with different return periods (Boundary Layer Wind Tunnel report, 2008)

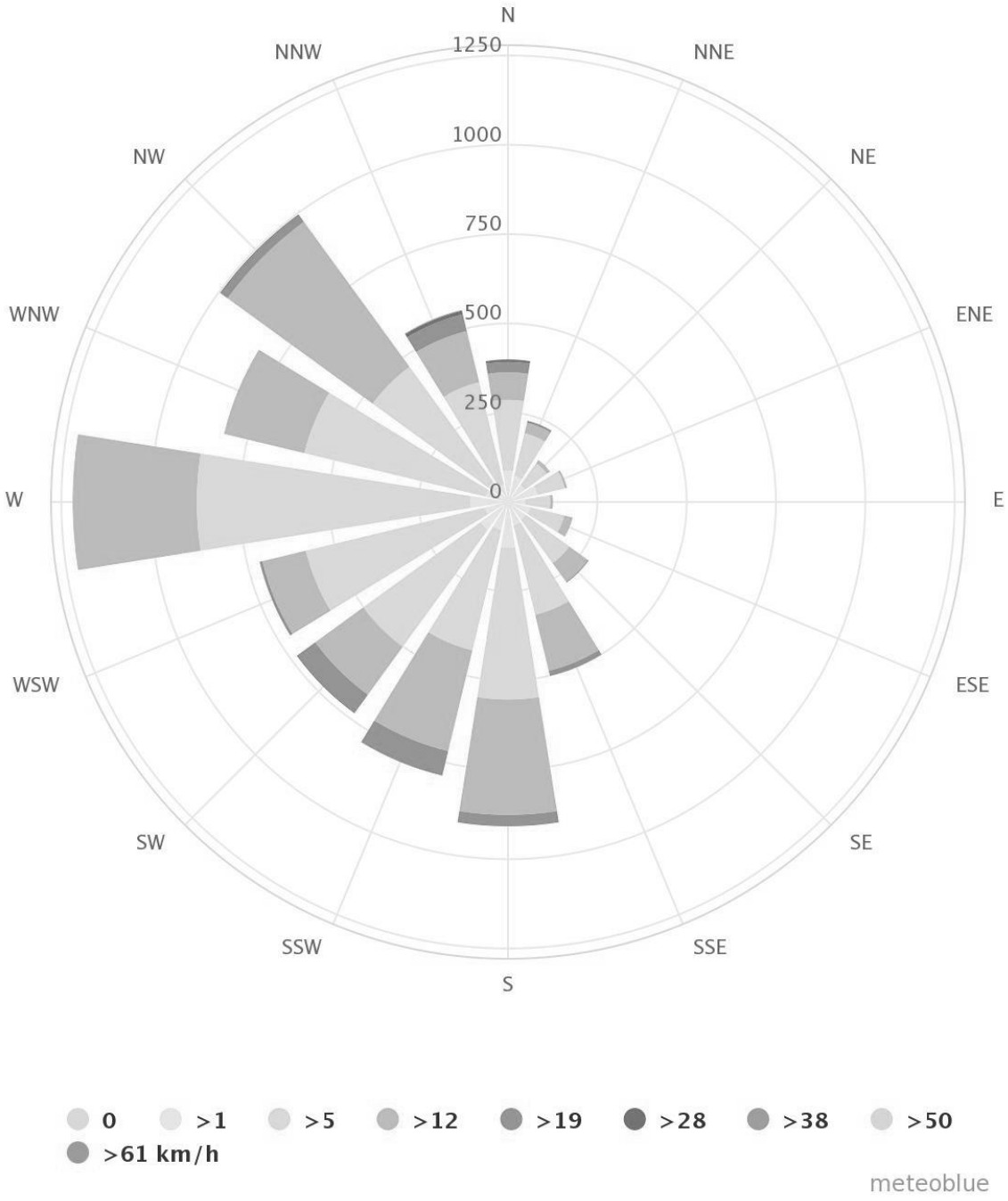

Fig. 2- 5: Hourly- Mean wind speeds with different return periods (Boundary Layer Wind Tunnel report, 2008)

2.3.3 Wind tunnel pressure test model

A rigid model was built for the building with a 1:500 scale and a pressure test was conducted in the Boundary Layer Wind Tunnel (BLWT) facility at the University of Western Ontario. **Fig. 2- 6** shows the pressure test model built for the building. Local pressure measurements were taken at 10° intervals for the full 360° azimuth range, at 400 samples per second for 26 seconds (equivalent to about 2.5 samples per second for one hour in full scale). Azimuths are measured from true north where 0^o is the north, 90^o is the east, 180^o is the south and 270^o is the west direction. Pressure Coefficient values from 114 pressure taps distributed along different elevations of the modelled building were recorded and integrated to evaluate wind story forces according to (Alan Davenport Wind Engineering Group, 2007).

A detailed proximity model of the surrounding city was built in block outline from Styrofoam for a radius of approximately 750 m. The building model and the proximity model were rotated to simulate different wind directions with the upstream terrain being changed as appropriate. The upstream terrain was modelled using generic roughness blocks and turbulence-generating spires to produce wind characteristics representative of those at the project site. The model profiles are good representations of the expected full-scale wind speed variation with height but deviate somewhat from that expected in full scale. To account for this, the reference wind speed measured in the wind tunnel has been adjusted to ensure that the roof-height wind speeds match the expected full-scale values according to Mara et al. (2008).

Fig. 2- 6: Pressure test model tested at the BLWT (Boundary Layer Wind Tunnel report, 2008)

2.3.4 Evaluation of wind forces from wind tunnel data

Time-history pressure coefficient values (C_p) were taken from wind tunnel results to evaluate story forces resulting from wind loading. Pressure coefficients are referenced to the reference height dynamic pressure which is calculated using this expression qref =1/2.ρ.$V_{ref}^{\ 2}$ according to Mara et al. (2007), where ρ = air density (1.225 kg/m^3) and V_{ref} is the mean-hourly wind speed at reference height. Thus the pressure coefficients are defined as C_p = Pressure / q_{ref}, where the pressure represents the pressure at the tap relative to the undisturbed reference static pressure. Tributary areas are calculated for each pressure tap for different elevations of the building, and then areas are resolved in the horizontal-X and vertical-Y directions of the building by angle (Θ) to account

for the inclination of the building with respect to the true north. The following equations were used to evaluate the wind force at each pressure tap elevation:

$$F_x = 1/2.\rho.V_{ref}^{\,2}.C_p.\ \text{Area}_{\text{Trib}}.\ \text{Cos}\ (\Theta)$$

Where Θ is the angle between the normal to each face of the building and the positive X-axis and $\text{Area}_{\text{Trib.}}$ is the tributary area of each pressure tap.

$$F_y = 1/2.\rho.V_{ref}^{\,2}.C_p.\ \text{Area}_{\text{Trib}}.\ \text{Cos}\ (\Phi)$$

Where Φ is the angle between the normal to each face of the building and the positive Y-axis.

This procedure is done for all C_p values in the time domain to form a time-history for story forces. The duration of the test was 1 hour in full-scale applied at a rate of 2.5 samples per second, with 14000 time steps and a time increment $\Delta t = 0.285$ sec. After evaluating wind forces in the two orthogonal directions for the 9 pressure tap rings installed at different elevations of the building, these forces are converted to story forces acting at the center of geometry of each story. Pressure tap elevations are divided into clusters dividing each force acting on a ring of pressure tap ring on the adjacent stories. **Fig. 2- 7** shows wind force time histories for groups of stories (story 1-7) nearest to its adjacent pressure tap ring. The figures showing time history story forces for the rest of the stories are provided in Appendix A.

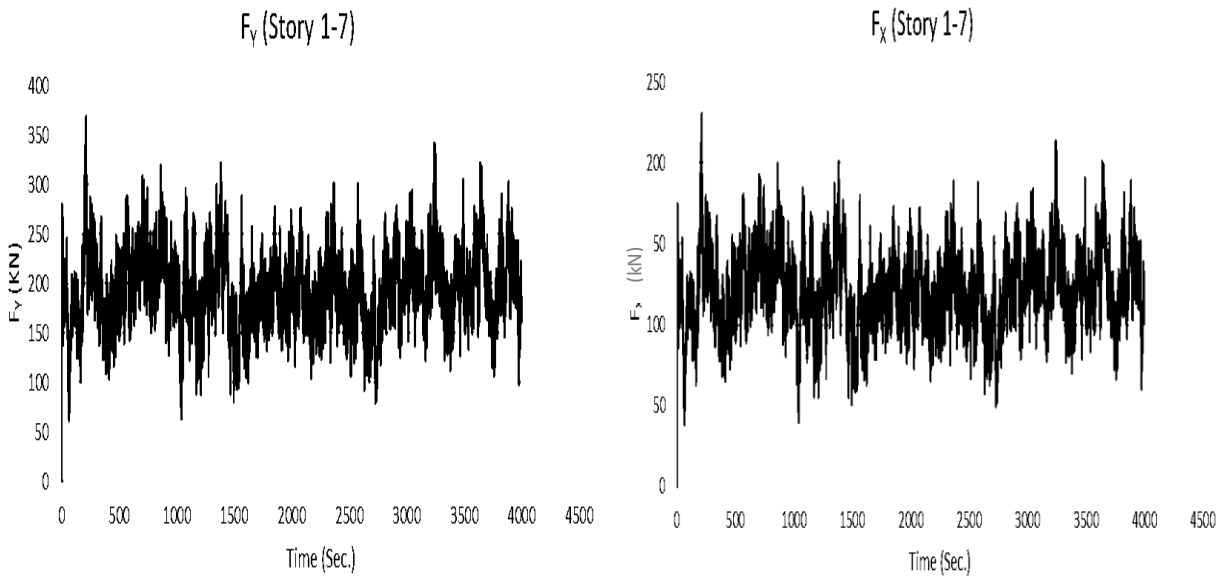

Fig. 2- 7: Story forces for stories 1-7

2.4 Step II: Finite Element Analysis

A 3D Finite Element model was developed for the building using ETABS software to evaluate mode shapes and natural periods of the structure, and conduct dynamic time- history analysis. Shear walls were modelled as shell elements in the preliminary stages just for running linear analysis, as computational run time was not an issue in this stage. Floor slabs were modelled as rigid diaphragms according to CSI Analysis Manual (2015). All walls and lateral load resisting system elements were fixed at the foundation level. Mass source was taken as the dead load in addition to the superimposed dead load on the slabs and a portion of the live load that is 25%. **Fig. 2- 8** shows plan view of the typical story of the building.

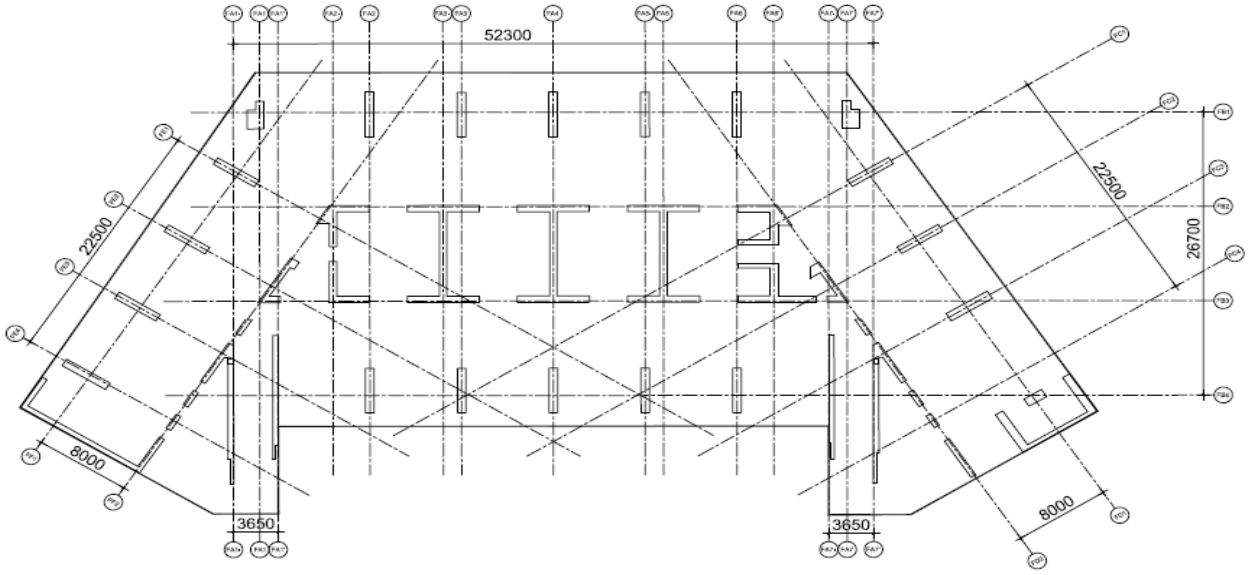

Fig. 2- 8: Plan view of the typical story of the building

Time history analysis is conducted to evaluate the dynamic response of the structure to an arbitrary loading. The dynamic equilibrium equation to be solved is given by:

$$K\,u(t) + C\,\dot{u}(t) + M\,\ddot{u}(t) = r(t)$$

Where K is the stiffness matrix; C is the damping matrix; M is the diagonal mass matrix; u, $\dot{u}$ &, and $\ddot{u}$ are the displacements, velocities and accelerations, and r is the applied load. ETABS software is used in this study to solve the dynamic equilibrium equation and evaluate the total responses of the structure. Damping ratio is taken as 1% of critical damping and the time step Δt is taken as 0.285 sec, which is the original time step of the wind record. Newmark method is used for performing direct-integration time history analysis with $\gamma = 0.5$ and $\beta = 0.25$.

Table 2- 1 shows modal analysis results in terms periods and mass participation factor, considering the first 20 modes. Mass participation factor represents the amount of the structure mass that contributes to each mode, so a mode with a large mass participation factor is usually a significant contributor to the structure response. Modal analysis results show that the structure's fundamental period is 10.88 sec., and the first mode is mainly governed by the torsion direction with an 83.5% mass participation ratio. As for the second mode, it is a transitional mode in Y-direction with 88.5% mass participation ratio and the third mode is governed by translation in X-direction with a mass 93.9% participation ratio. **Fig. 2- 9** shows the first three mode shapes.

Table 2- 1: Modal Analysis Results with original cross sections

Modal Analysis Results before reducing cross sections				
Mode	**Period**	**UX**	**UY**	**RZ**
	sec	%	%	%
1	10.882	5.9	10.6	83.5
2	10.376	0	88.5	11.5
3	7.38	93.9	0.9	5.2
4	2.657	2.1	12.7	85.2
5	2.557	3.4	82.7	13.9
6	2.198	94.1	4.6	1.2
7	1.21	43.7	1	55.3
8	1.13	16	63.1	20.9
9	1.045	40.2	35.9	23.9
10	0.752	65.7	0.6	33.7

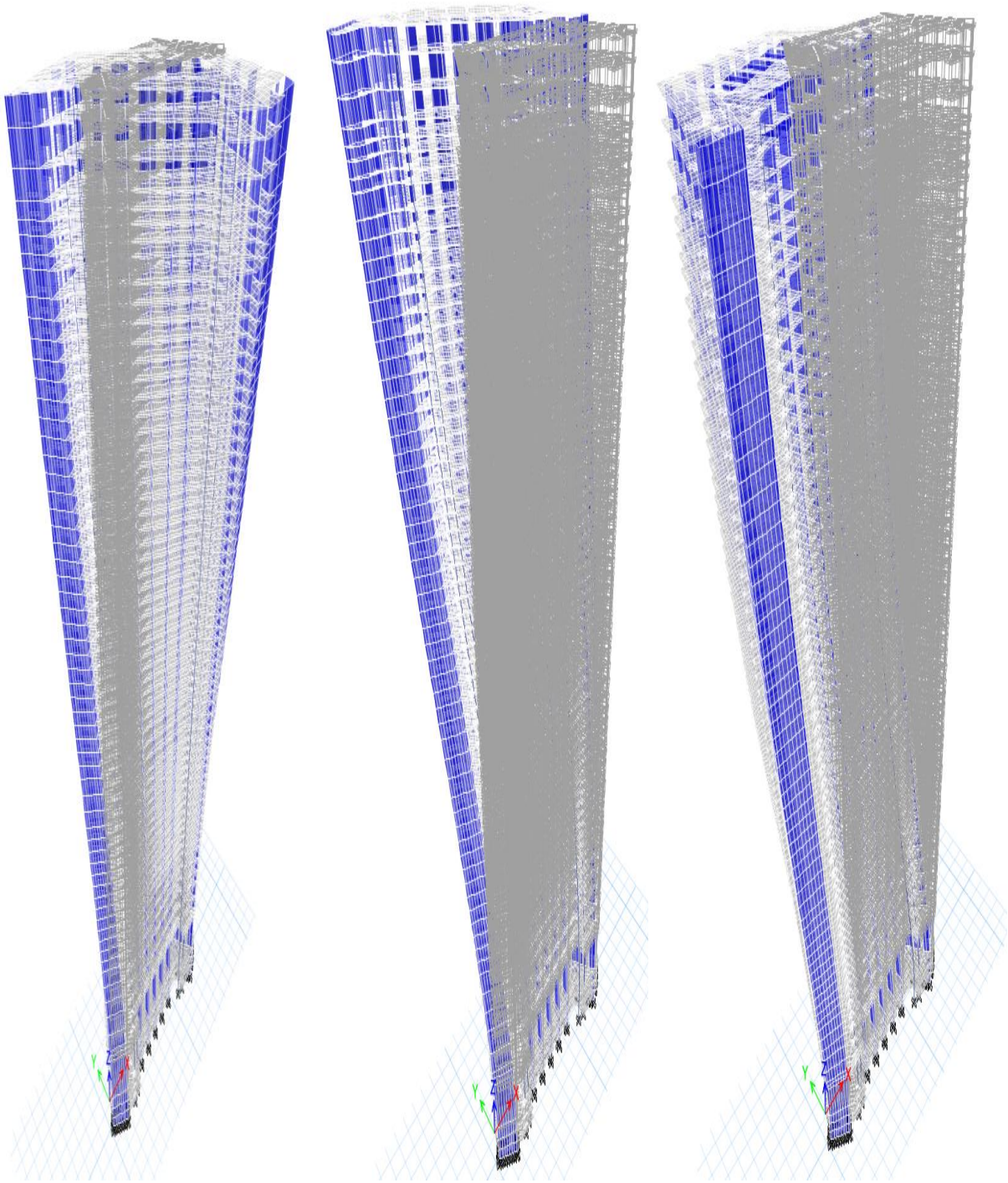

Mode 1 **Mode 2** **Mode 3**

Fig. 2- 9: The first three mode shapes of the building

2.5 Step III: Evaluate response total, Mean+Background and resonant component ($V_T(t)$, $V_{Mean+BG}$, V_R)

2.5.1 Dynamic Time History Analysis

The third step in the flowchart involves running linear dynamic time history analysis applying wind forces time-histories on the center of geometry of each story diaphragm to get the structure total response to wind loading (V_T (t)). **Fig. 2- 10** and **Fig. 2- 11** show the time history for base shear in the X and Y directions.

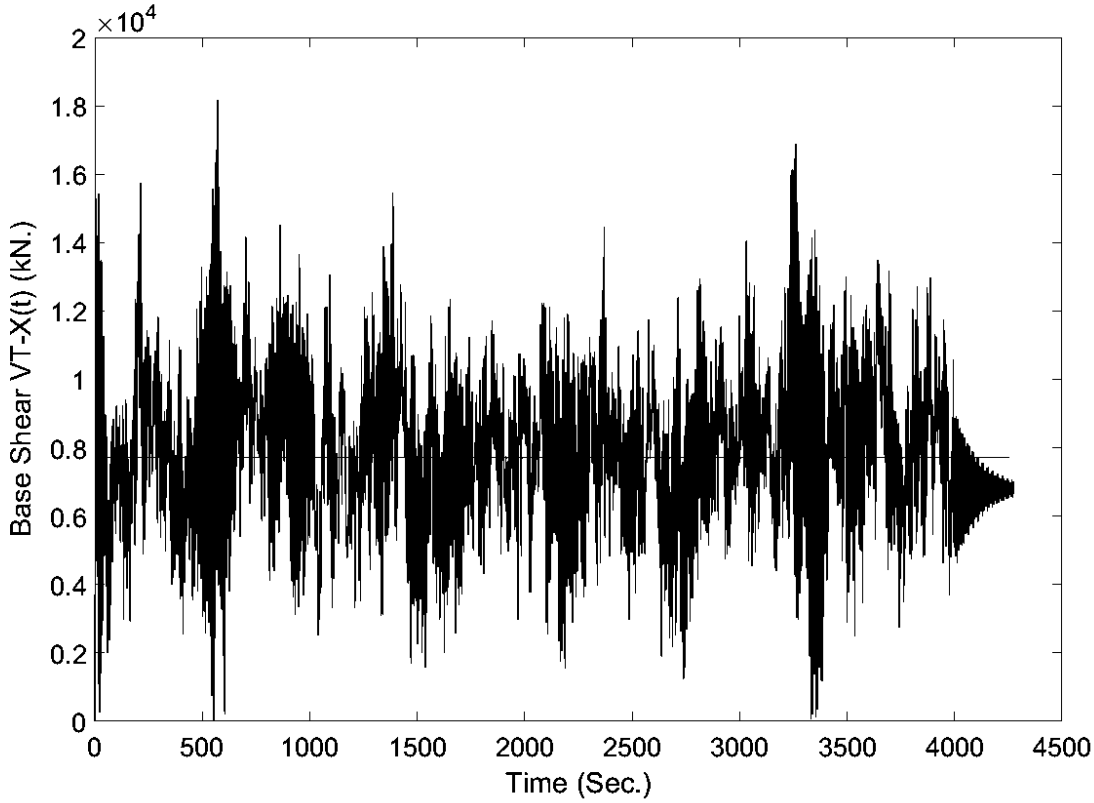

Fig. 2- 10: Total Base Shear VT-X (t)

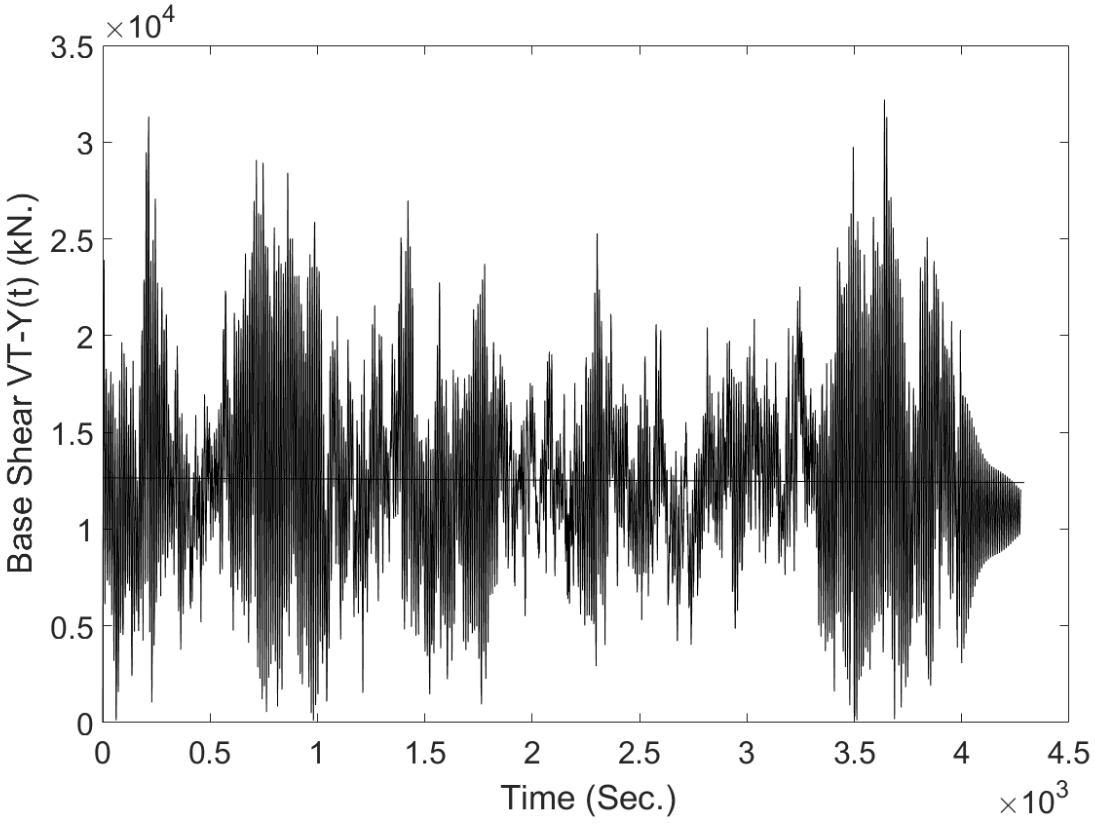

Fig. 2- 11: Total Base Shear VT-Y (t)

2.5.2 Step IV: Decomposition of Wind Response into Mean, Background and Resonant component

The second step in the analysis involves decomposition of the wind response. Wind response is divided into a mean part, and a fluctuating part that can be decomposed into background (quasi-static) and the resonant response. The background component refers to the quasi-static response of the fluctuating part of wind response which occurs when wind load frequency is lower than the natural frequency of the structure. On the other hand, the resonant component refers to the additional dynamic amplification of the response according to (Holmes, 2001).

Several approaches can be used to decompose the fluctuating part into Background (quasi-static) and Resonant. For example, most codes simplify this part into the so-called “Gust Response

Factor" and this factor should be multiplied by the quasi-static loads resulting from applying the loads as if the building was rigid as per NBCC (2010). In this study, the methodology presented for separating the resonant component from the background (quasi-static) component is as follows: First, Quasi-static analysis is done applying wind load with an artificial large time step which is 11 sec (≈ 40 times the original time step) to capture the mean + background part of the response $V_Q(t)$. Then resonant component $V_R(t)$ is evaluated by linear subtraction of $V_Q(t)$ from the total response $V_T(t)$.

To illustrate this separation procedure, the power spectral density function for the fluctuating wind response (base shear Vx(t)) with different time steps and the corresponding frequencies are calculated and plotted using a Fast Fourier Transform application. The procedure is repeated using different time steps in an incremental manner, using the multiples of the original time step, which is 0.285 sec. **Fig. 2- 12** shows the spectral density function for the fluctuating part of the response using different time steps.

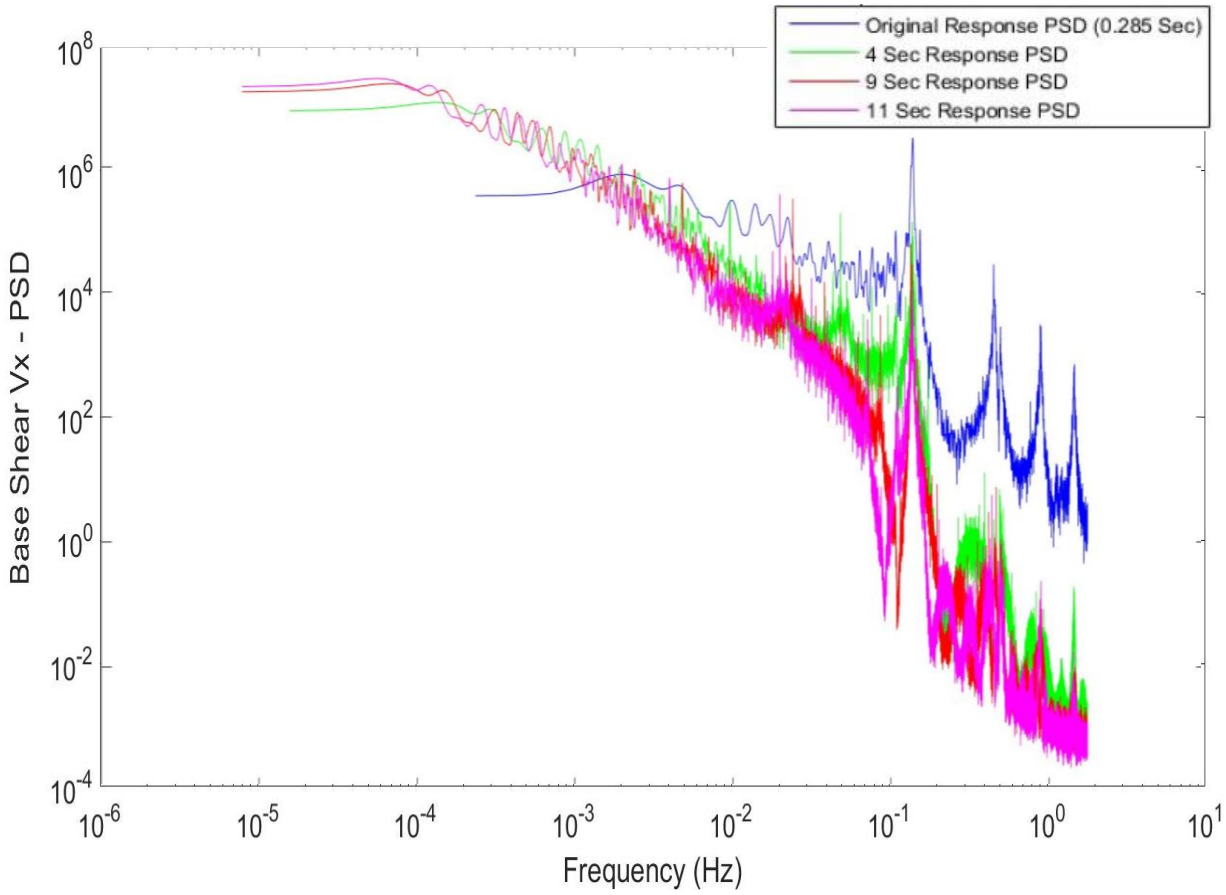

Fig. 2- 12: Spectral density function for base shear Vx-T

It can be observed from **Fig. 2- 12** that the resonant part represented in the peaks in the response starts to decrease gradually as time step increases. The PSD is plotted for each response resulting from each time step until the peaks in the resonant part eventually diminishes in the last trial, which was the response for $\Delta t = 9$ sec. Sensitivity analysis is performed on the peak base shear of each response until the variation between the peak base shear values corresponding to two different time steps converges. Convergence is achieved when using $\Delta t = 11$ sec and the difference between the

peak base shear using Δt =11 sec. and Δt= 9 sec. is found to be 1.5 %. **Fig. 2- 13** shows the peak base shear values plotted against the time step value.

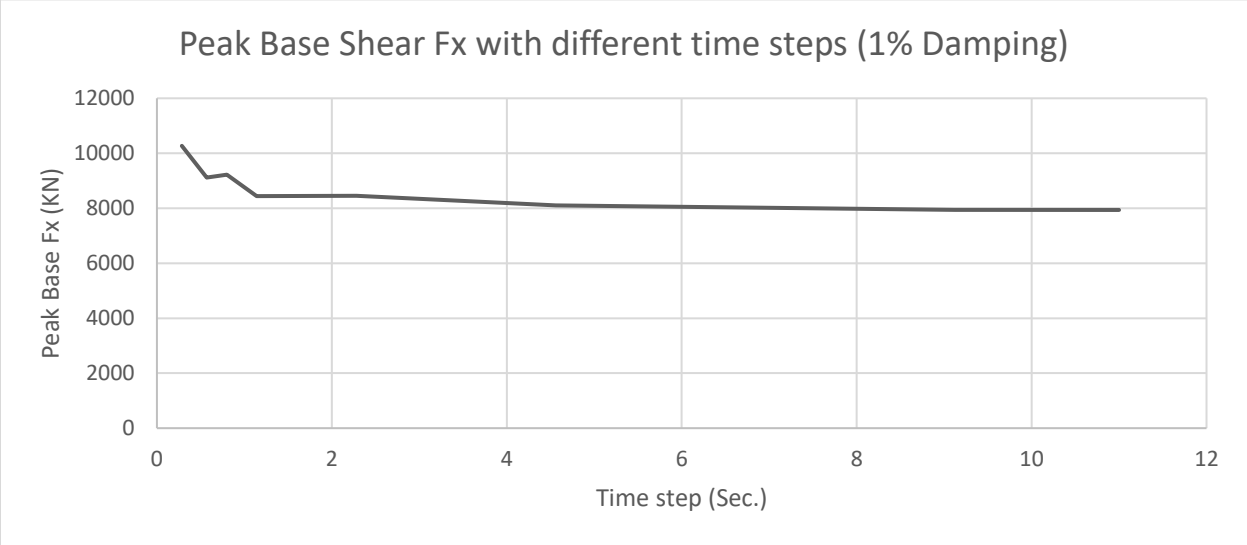

Fig. 2- 13: Base shear values versus different loading time steps

The final time step Δt used for running quasi-static analysis is 9 sec. This analysis is conducted to capture mean + background components of the response separately. Newmark method is used for performing direct integration time history analysis, with the same parameters used in the case of full dynamic analysis. Damping ratio is taken as 1% of critical damping. The mean + background response is plotted against time. Dynamic amplification factor (DAF) is evaluated by dividing the peak total base shear/ peak quasi-static base shear. DAF is found to be 1.37 for X direction (V_x) and 1.51 for Y direction (V_Y). **Fig. 2- 14** and **Fig. 2- 15** shows the time history for mean + background base shear in X and Y directions respectively.

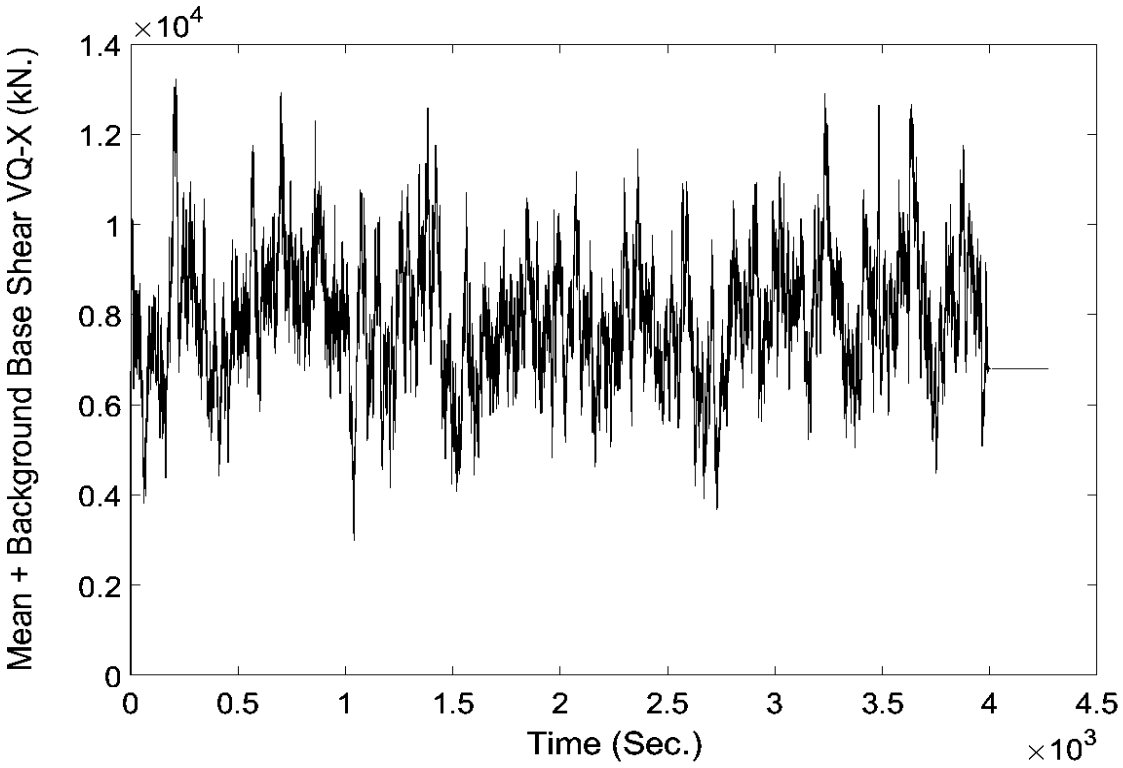

Fig. 2- 14: Mean + Background Base Shear VQ-X (t)

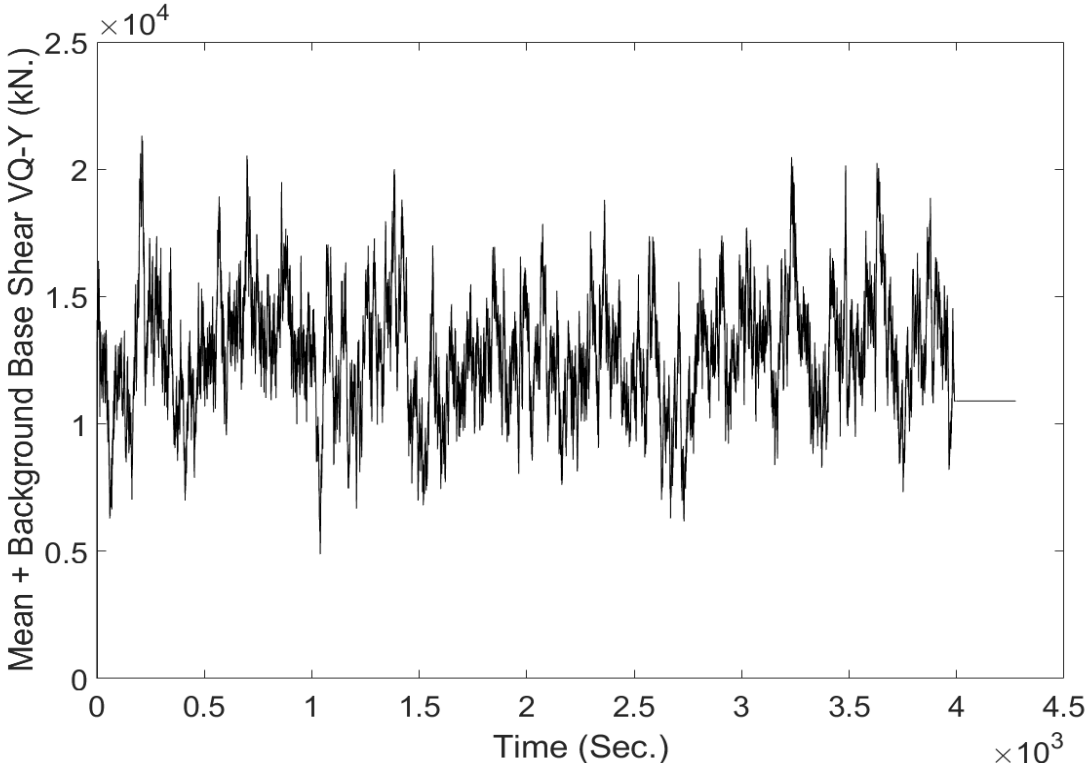

Fig. 2- 15: Mean + Background base shear VQ-Y (t)

Resonant component of the base shear is evaluated by linear subtraction of the mean + background base shear $V_Q(t)$ from the total base shear $V_T(t)$. **Fig. 2- 16** and **Fig. 2- 17** show the time histories of base shear in X and Y directions respectively.

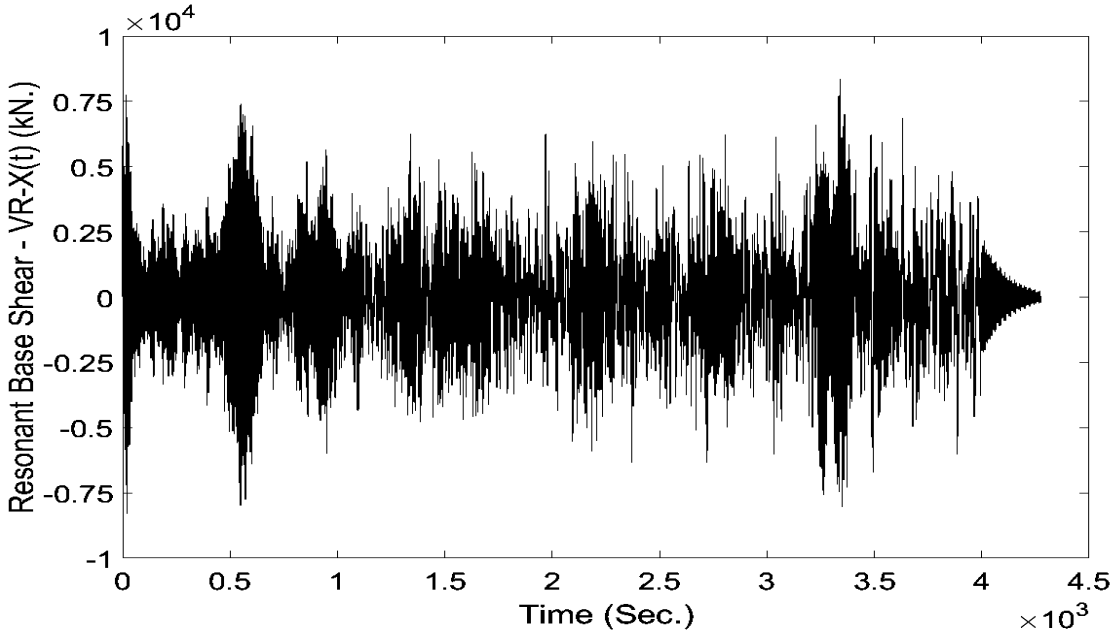

Fig. 2- 16: Resonant Base Shear VR-X (t)

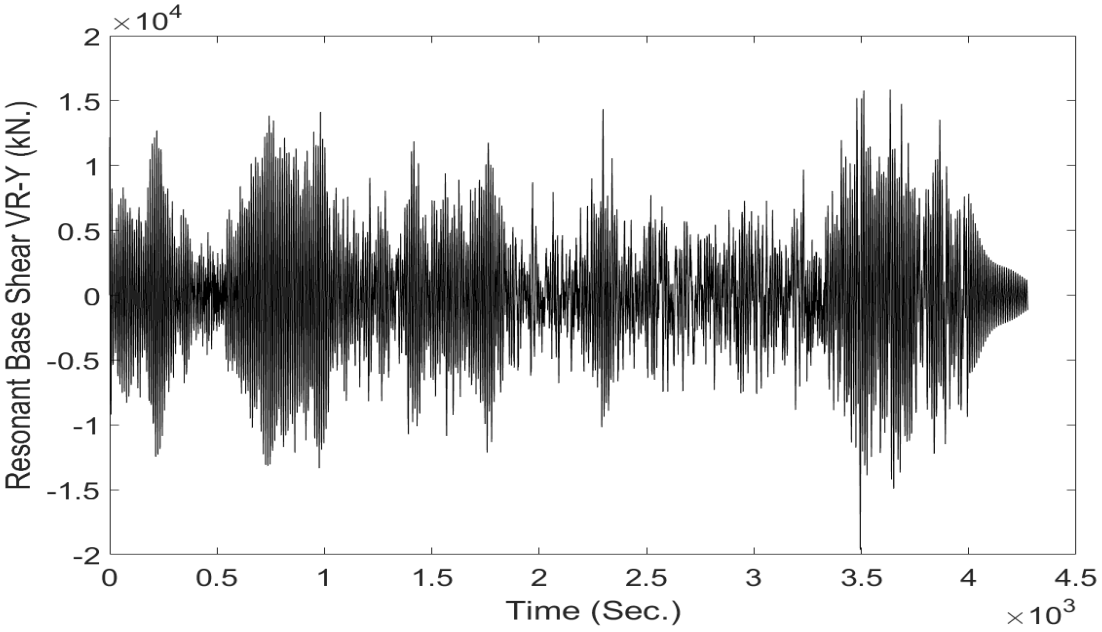

Fig. 2- 17: Resonant Base Shear VR-Y (t)

2.6 Step V: Ductility based approach – [VT-I (t)]

2.6.1 Reducing Wind Resonant Component by "R" factor

The next step in the flowchart involves reducing wind resonant component by a factor "R". A new set of wind loads are applied on the structure and accordingly, redesign of the lateral load structural system under the reduced load is conducted. **Fig. 2- 18** and **Fig. 2- 19** show plots for time history of reduced resonant component of wind response, which yielded the new straining actions to carry out redesign for shear walls. The "R" factor is given the value of 2 in this study.

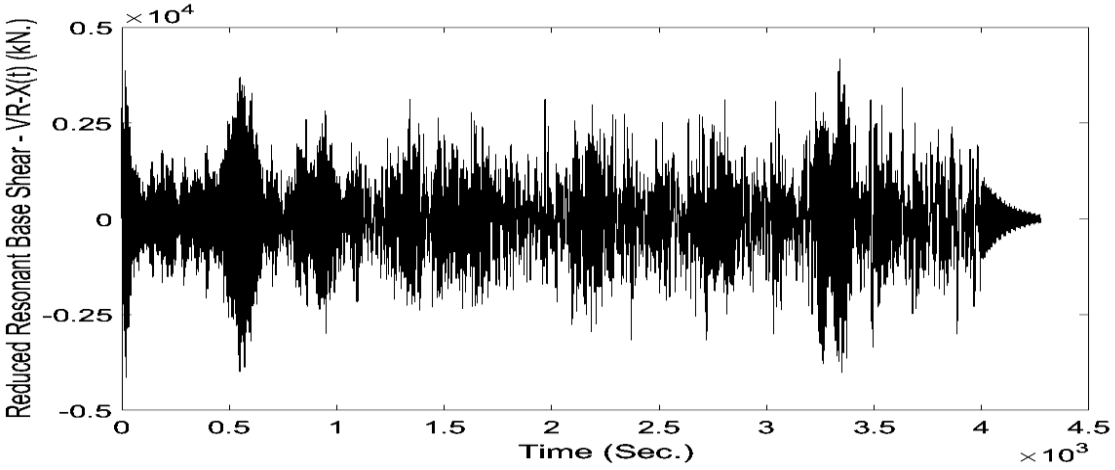

Fig. 2- 18: Reduced resonant base Shear VR-X (t)/R

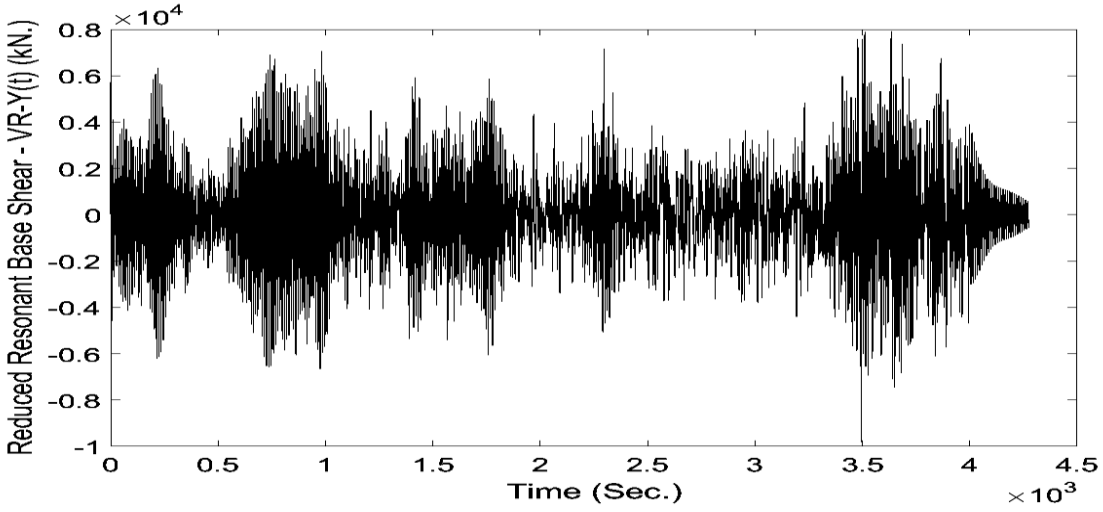

Fig. 2- 19: Reduced resonant base shear VR-Y (t)/R

Fig. 2- 20 and **Fig. 2- 21** show the new applied base shear which is denoted by VT-I (t) which is the summation of Mean + Background components [V_{Mean}+V_{BG}(t)] and the reduced resonant component [V_R(t)/R].

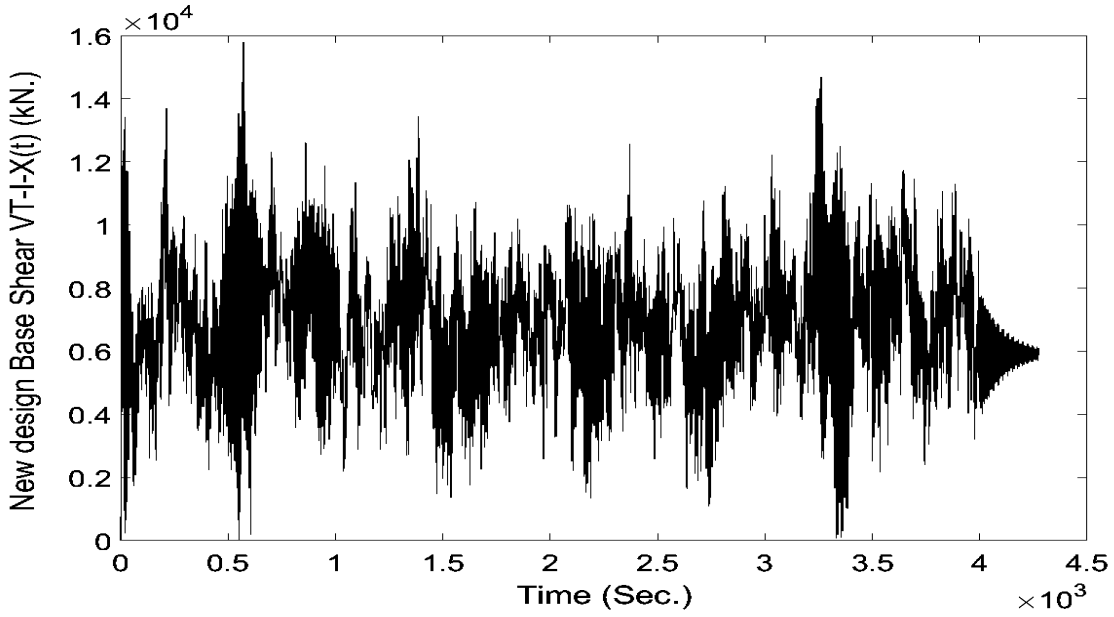

Fig. 2- 20: New design base shear (VT-I-X (t))

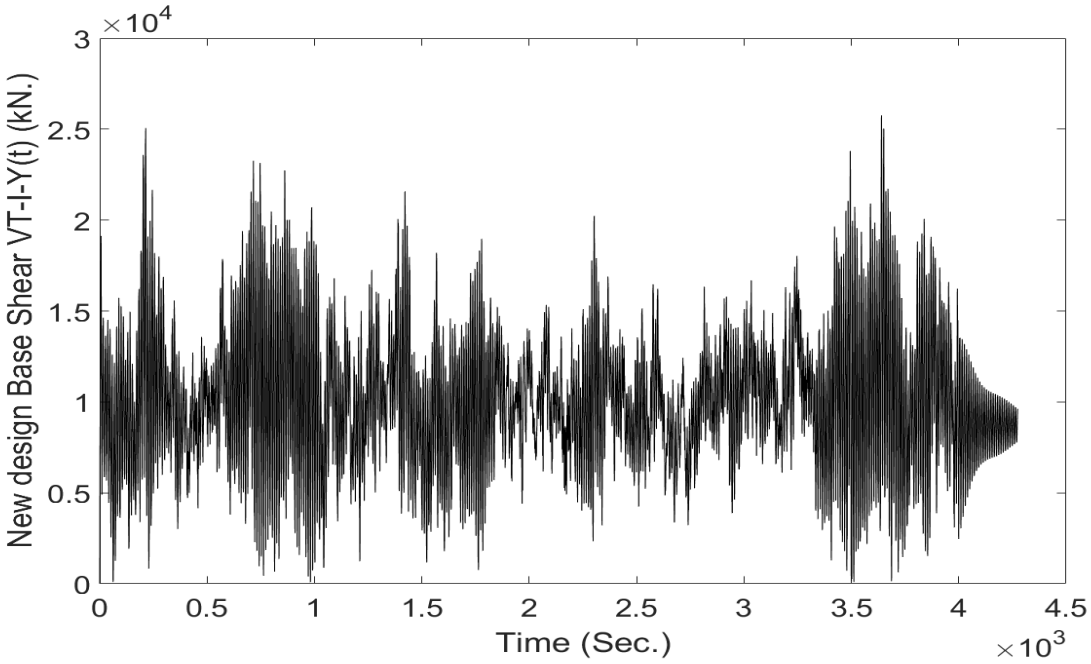

Fig. 2- 21: New design base shear (VT-I-Y (t))

2.6.2 Redesign of the concrete shear walls under the new set of loads

The reduction procedure is done on each wall individually in terms of their bending moments. Total base moment on each shear wall is separated into Mean + Background part (M_Q) and Resonant part (M_R). The new set of design straining actions are resulting from adding Mean + background bending moment (M_Q) to the reduced resonant bending moment (M_R.). **Fig. 2- 22** shows the building layout and shear wall modules under study.

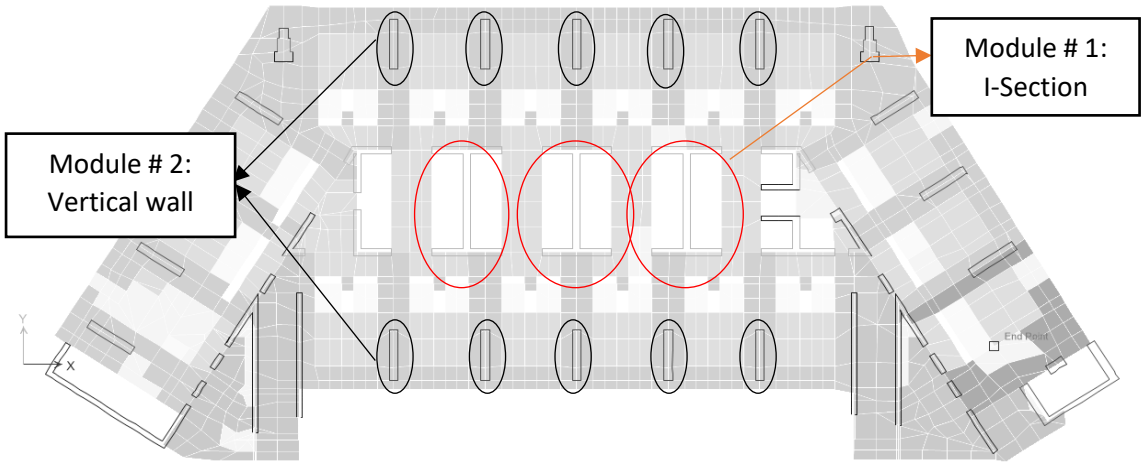

Fig. 2- 22: Building plan layout

Torsion is not considered in this case as torsional effect on shear walls is studied, and it is found that the governing case in design is the bending moment. Check of shear is performed on each shear wall and torsional effects are not the governing case in shear design. Another reason for not

taking torsion into acouunt is that the objective of this study is just the proof of concept; which is the applicability of ductility-based approach on shear walls subjected to wind loads.

Table 2- 2 shows the summary of reduction procedure and the new design moments on shear wall modules.

Table 2- 2: Summary of reduction procedure on shear walls' straining actions

Bending moments on Shear Walls:		**(R = 2)**
Module # 1: I-Section	(Thickness = 35 cm)	
Total Moment =	**448626**	kN.m
Quasi-Static (M +BG) =	258982	kN.m
Resonant =	189644	kN.m
Reduced Resonant =	94822	kN.m
New Moment Applied =	**353804**	kN.m
Section is reduced from 35 cm to 28 cm		
Module # 2: Vertical Wall	(Thickness = 50 cm)	
Total Moment =	**21280**	kN.m
Quasi-Static (M +BG) =	12362	kN.m
Resonant =	8918	kN.m
Reduced Resonant =	4459	kN.m
New Moment Applied =	**16821**	kN.m
Section is reduced from 50 cm to 35 cm		

Results show that due to reducing wind resonant component by a factor of 2, moments on shear walls were reduced by about 22%, and accordingly there was a saving in concrete volume of affected shear walls by a percentage ranging from 20-25%.

2.7 Effect of reducing wind resonant component on Structure Dynamic characteristics.

2.7.1 Modal analysis results of structure with reduced cross sections:

The effect of reducing shear wall concrete dimension on global behavior of the structure in terms of fundamental periods and response to wind loading is studied. It is found that as a result of reducing walls' cross sections, fundamental period of the structure changed from 10.8 sec to 11.5 sec. **Table 2- 3** presents a comparison between mode shapes and fundamental periods before and after reduction. The fundamental period of the structure changed from 10.88 sec to 11.5 sec with only 7% increase.

Table 2- 3: Modal analysis results before and after reduction

Modal Analysis Results before reducing cross section					Modal Analysis Results after reducing cross sections				
Mode	Period	UX	UY	RZ	Mode	Period	UX	UY	RZ
	sec					sec			
1	10.882	5.9	10.6	83.5	1	11.563	6.4	5.6	88
2	10.376	0	88.5	11.5	2	10.956	0	93.7	6.2
3	7.38	93.9	0.9	5.2	3	7.527	93.5	0.6	5.9
4	2.657	2.1	12.7	85.2	4	2.909	3.9	2.3	93.8
5	2.557	3.4	82.7	13.9	5	2.71	1.5	95.4	3.1
6	2.198	94.1	4.6	1.2	6	2.268	94.3	2.3	3.4
7	1.21	43.7	1	55.3	7	1.287	4.1	0.3	95.5
8	1.13	16	63.1	20.9	8	1.207	50.5	48.2	1.3
9	1.045	40.2	35.9	23.9	9	1.14	45.2	51.4	3.3
10	0.752	65.7	0.6	33.7	10	0.779	54.7	0.3	44.9

2.7.2 Dynamic time history analysis of the structure with reduced cross sections:

Step III in the flowchart is repeated and full dynamic time history analysis is conducted again on the building with reduced wall cross sections, applying the original time history load. The results show that the peak base shear in the two orthogonal directions did not change much; there is about 4% change only. **Fig. 2- 23** and **Fig. 2- 24** show the base shear in X and Y directions after reducing shear wall cross sections.

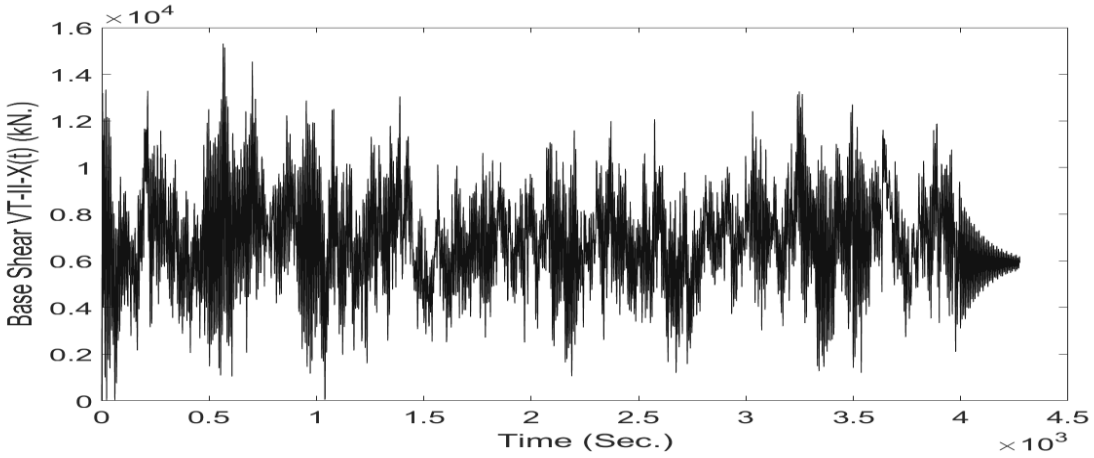

Fig. 2- 23: Total Base Shear VT-X (t) after redesign

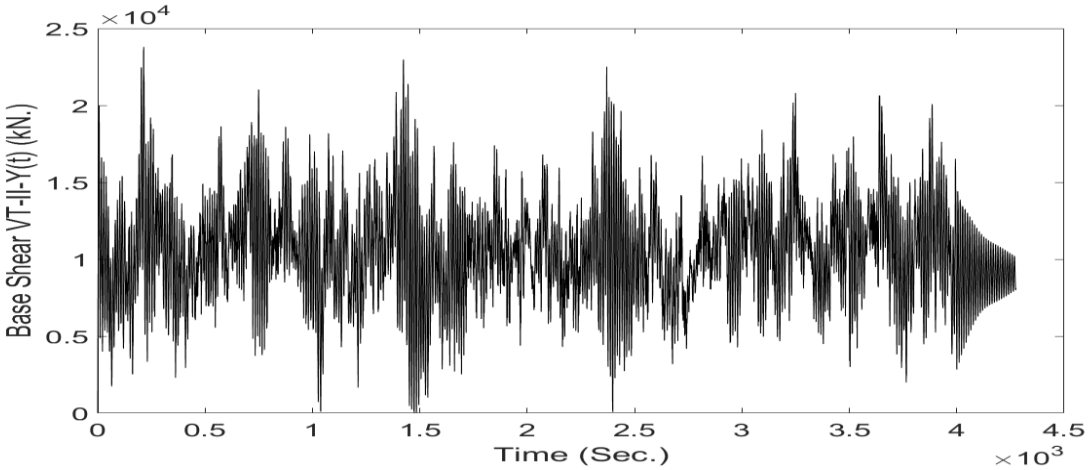

Fig. 2- 24: Total Base Shear VT-Y (t) after redesign

Therefore, it can be concluded from the previous comparisons, that reducing wind resonant component and redesigning the lateral load resisting system based on the reduced load did not have a major effect on the structural global behavior in terms of fundamental period and responses.

Table 2- 4 summarizes the comparison between the structure's dynamic characteristics before and after reduction. Results show that reduction of wind resonant component did not have a major effect on base shear in X and Y directions and dynamic amplification factor.

Table 2- 4: Base Shear values before and after reduction

	Structure with initial cross sections V_T (t)	**Reduced applied load – V_{T-I} (t) = (V_M+V_{BG}+V_R/2)**	**Structure with reduced cross sections V_{T-II} (t)**
Base Shear V_X (kN)	18170	15715	15435
Base Shear V_Y (kN)	32200	26760	24940
DAF for V_x	1.37	-	1.33
DAF for V_y	1.51	-	1.44

2.8 Parametric study on changing "R" factor and its effect on structure dynamic characteristics

In this section, a parametric study is presented, trying different reduction factors on wind resonant component. Shear walls are redesigned based on the reduced straining actions in each case. The analysis is done again under the reduced set of loads. The maximum reduction factor employed here is R=3 as it's not expected that the load reduction factors will be as its counterpart in seismic design where load factors can range between 2.8 and 5.6. The fundamental period of the structure is plotted against different reduction factors as shown in **Fig. 2- 25** Base shear is also evaluated in each case and plotted against the reduction factor as shown in **Fig. 2- 26**.

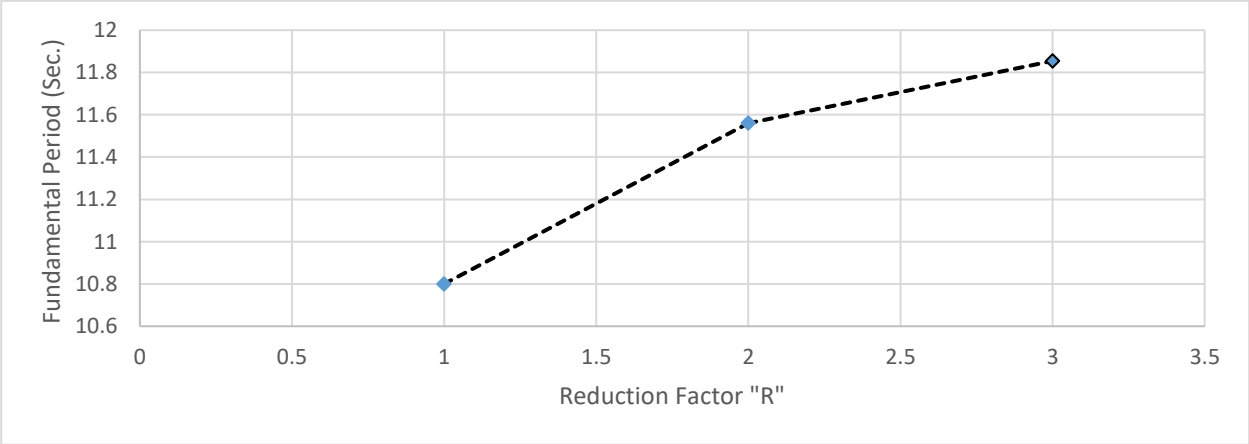

Fig. 2- 25: Fundamental Period values with different reduction factors

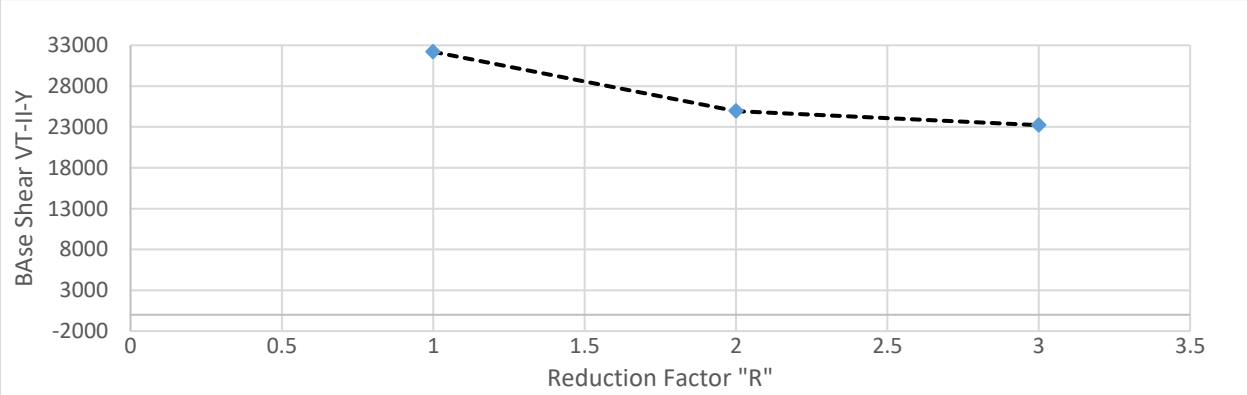

Fig. 2- 26: Base Shear values with different reduction factors

CHAPTER 3

NON-LINEAR STATIC ANALYSIS FOR REDUCED REINFORCED CONCRETE SHEAR WALLS SUBJECTED TO EXTREME WIND LOADS

3.1 Introduction

It is concluded from chapter 2 that concrete shear wall modules are designed based on ductility design approach. Wind resonant component of the wind loading is reduced by a factor R=2. Accordingly, concrete shear walls are redesigned. This chapter examines the application of ductility-based approach on concrete shear walls of the building. Non-linearity is defined by assigning plastic hinges at potential locations along the shear wall, and defining moment rotation relationships for hinges as per (ASCE/SEI 41-13). Pushover analysis load patterns are obtained from linear time history dynamic analysis of the full building, applying shear force distribution on each wall individually. Displacement controlled pushover analysis is conducted.

Pushover load-displacement curves are obtained for each shear wall module, and ductility demand μ is evaluated as a result of using a load reduction factor of R = 2. Moment rotation curves for plastic hinges are evaluated and plastic rotation experienced by the walls are compared with plastic rotation limits for each target performance level, Immediate Occupancy (IO), Life Safety (LS) and Collapse Prevention (CP). Furthermore, a parametric study is conducted on the level of ductility of concrete shear walls and its effect on the plastic hinge responses and target performance level reached. **Fig. 3- 1** shows the flowchart for nonlinear analysis conduced in this chapter.

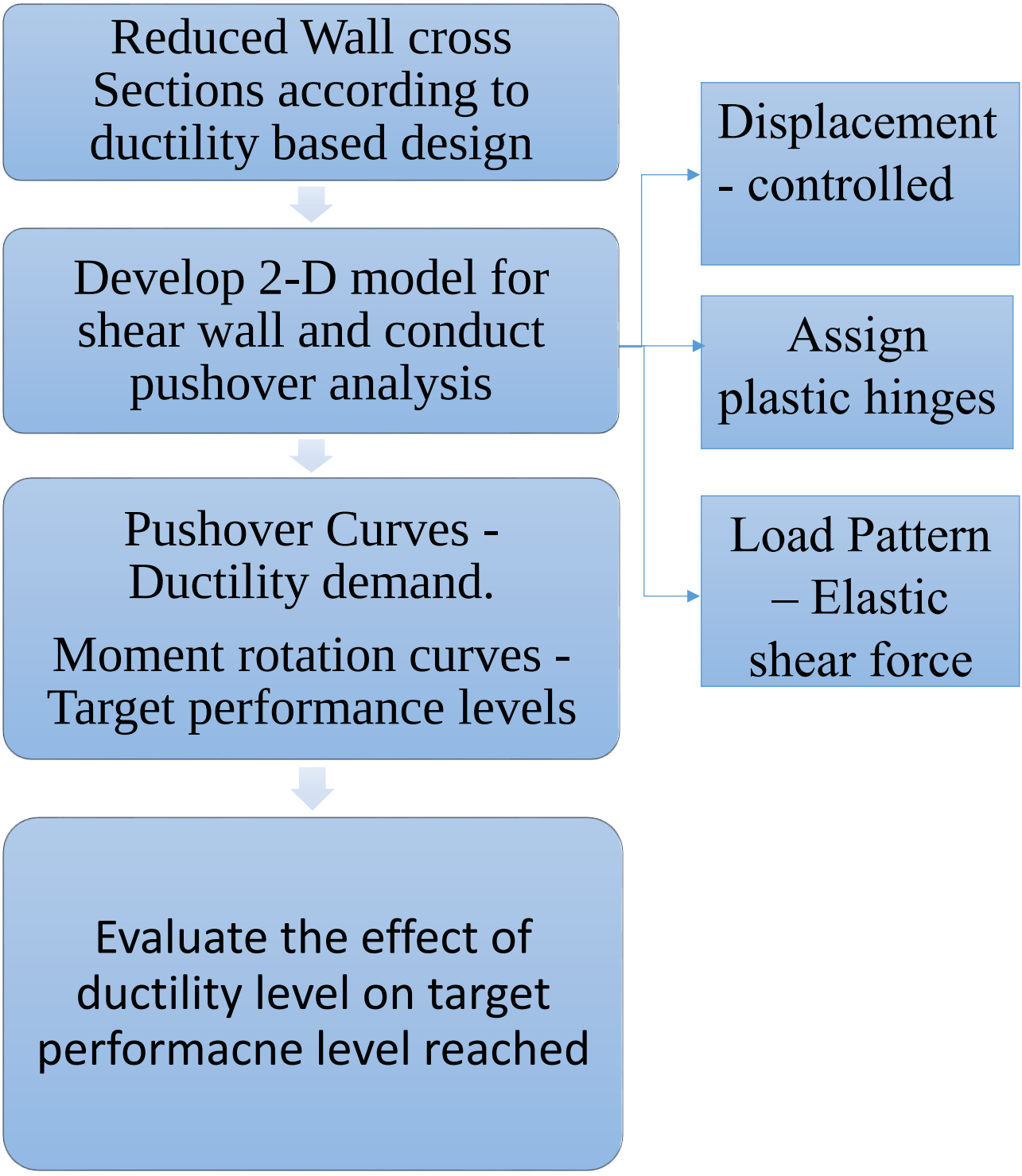

Fig. 3- 1: Flowchart for nonlinear analysis of reduced shear walls

3.2 Methodology:

3.2.1 Reduced shear wall cross sections based on ductility design:

First, Reduced shear wall cross sections (as a result of reducing wind resonant component by R=2) are obtained from the redesign procedure done in chapter 2. The peak bending moment is extracted from linear analysis of the full model of the building. **Fig. 3- 2** and **Fig. 3- 3** show the time history base shear for I-Section shear wall and vertical wall 4200 mm long.

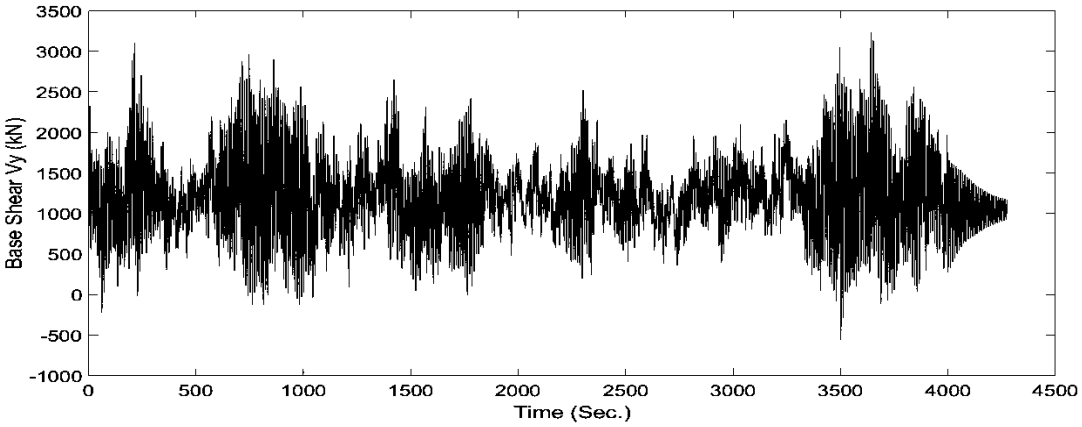

Fig. 3- 2: Base Shear Time History for I-section wall from linear analysis

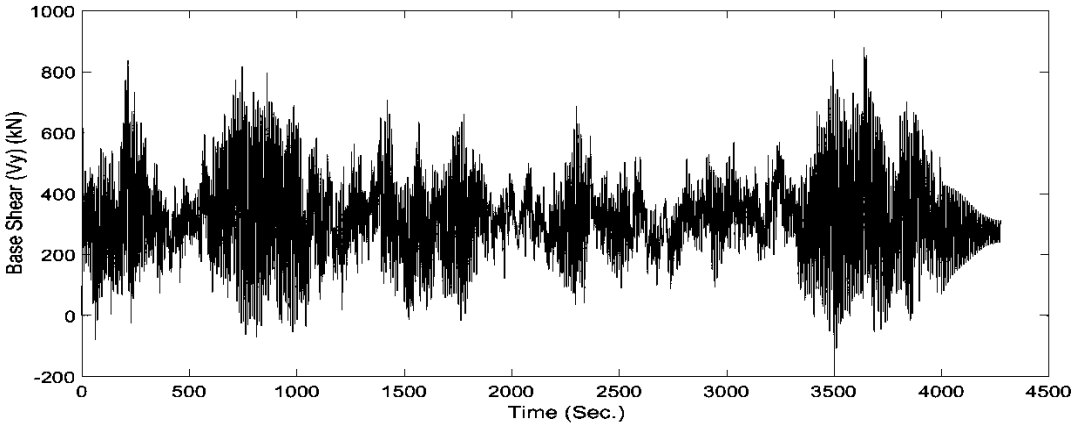

Fig. 3- 3: Base Shear Time History for Vertical wall (4200 mm) from linear analysis

3.2.2 2-D modelling of shear walls and static pushover analysis

Second, Pushover analysis conducted in this case is displacement-controlled analysis, where the member is loaded until it reaches a target displacement and strength degradation gradually starts occurring, and eventually the member reaches collapse. **Fig. 3- 4** shows the typical force – displacement pushover behavior of a reinforced concrete member.

Zone 1 in the pushover curve that lies between points A and B represents the linear zone. Between points B and C. Zone 2 is the zone where concrete start to spall and strain hardening takes place, which, in well-confined sections, can be associated with strain hardening of the longitudinal reinforcement and an increase in strength from the confinement of concrete. After point C, is the zone where strength loss starts and member fails gradually until reaching collapse, which represents point D on the curve.

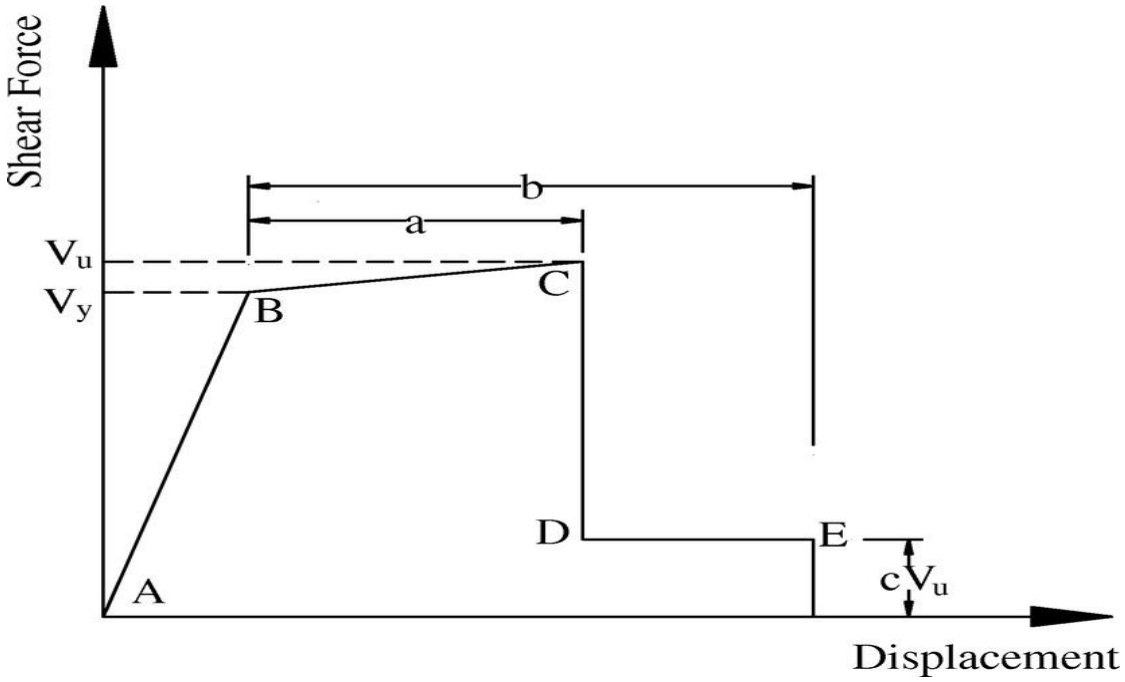

Fig. 3- 4: Typical backbone curve for reinforced concrete cross section. (FEMA 356)

The shear walls in this model are modelled using a set of frame elements, with each frame element assigned a concrete cross-section with defined steel reinforcement designed as per (ACI – 318). Boundary conditions are defined assuming that the wall is fixed at its base. Plastic hinge properties are assigned for different frame elements as per moment rotation curve parameters shown in **Table 3-1** (as per ASCE/SEI 41-13 – table 10-8, Modelling Parameters and Numerical Acceptance Criteria for Nonlinear Procedures - Reinforced Concrete Shear Walls). Defining concrete section properties, reinforcing steel, and shear reinforcement also, the modelling parameters and acceptance criteria are defined and the moment rotation backbone curves are plotted for the concrete cross-section depending on two parameters, the first one is $\frac{P}{Ag\ f'c}$ where P is the axial force, A_g is the gross area of the cross section and f'_c is concrete compressive strength. The other parameter is $\frac{Av}{bw.S}$ which represents the shear reinforcement of the section; where A_v is the shear reinforcement, b_w is the shear depth and s is the spacing of stirrups.

The backbone curve, as shown in **Fig. 3- 4**, consists of five segments. The first segment represents the linear zone until reaching yield (V_y), no deformation occurs in the hinge up to point B. Point C represents the ultimate capacity of the section for pushover analysis. Point D represents residual strength and point E represents total failure.

Modelling parameters and acceptance criteria are defined depending on the level of axial force P, the shear reinforcement A_v ,the shear width b_w and spacing of stirrups s. The parameter a which is the distance between points B and C on the backbone curve is a measure of the ductility of the section. **Table 3-1** shows the modelling parameters and numerical acceptance criteria for nonlinear

procedures as per (ASCE/SEI 41-13). The tabulated values are given for condition i sections (as per ASCE/SEI 41-13) for sections governed by flexural failure, which is the case for most shear walls. Rows are sorted in **Table 3- 1** from ductile to moderate to limited ductile as we go from top row to the bottom row.

Table 3- 1: Modelling Parameters and Numerical Acceptance Criteria for Nonlinear Procedures - Reinforced Concrete Shear Walls. (ASCE/SEI 31-41*)*

$\frac{P}{Ag\ f'c}$	$\frac{Av}{bw.S}$	a	b	c	IO (rad.)	LS (rad.)	CP (rad.)
≤ 0.1	≥ 0.006	0.035	0.060	0.2	0.005	0.045	0.060
≤ 0.1	= 0.002	0.027	0.034	0.2	0.005	0.027	0.034
≤ 0.1	< 0.002	0.010	0.010	0.0	0.003	0.009	0.010

For each rotational degree of freedom (bending) in the frame element, plastic hinges are assigned using a plastic moment – rotation behaviour. Degrees of freedom that are not specified remain elastic. Each plastic hinge is modeled as a discrete point hinge. All plastic hinge deformations whether displacement or rotation, occur within the point hinge.

As per ASCE/SEI 41-13, immediate occupancy Structural Performance Level is defined as post-hazard damage state in which only very limited structural damage has occurred. The basic vertical and lateral force resisting systems of the building retain nearly all of their pre-hazard strength and stiffness. The risk of life threatening injury as a result of structural damage is very low, and although some minor structural repairs may be appropriate, these would generally not be required prior to reoccupancy.

Table 3- 2 shows each structural acceptance criteria. ASCE/SEI 41-13 specifies the level of damage accompanied by each structural performance criteria. Immediate occupancy level is specified in the table, and overall damage for this structural performance level is explained. The overall damage life with no permanent drift occurring. Structures substantially retains its original strength and stiffness. Minor damages can occur in non-structural elements as facades, partitions and ceilings.

Table 3- 2: Damage Control and Building Performance Levels

Immediate occupancy (IO)	**Life Safety (LS)**	**Collapse Prevention (CP)**
No permanent drift – No loss in strength – Minor cracking occurs in facades.	Some permanent drifts occur – Minor loss in strength – Building may be beyond economical repair.	Large permanent drifts – Major loss in strength – Building is near collapse.

ETABS finite element software is used to do static pushover analysis for shear walls with reduced cross sections. Reduction was done based on the procedure described in chapter 2. The Linear model for elastic design was used as the baseline for non-linear analysis done in this part. Displacement-controlled Static pushover case is defined applying the load pattern as the shear force diagram resulting from elastic analysis of the section shown in **Fig. 3- 5** to **Fig. 3- 8**. The application of a larger load on the wall with reduced cross-section; i.e.: reduced capacity, it is expected that the member will experience inelastic actions and a certain level of ductility is reached.

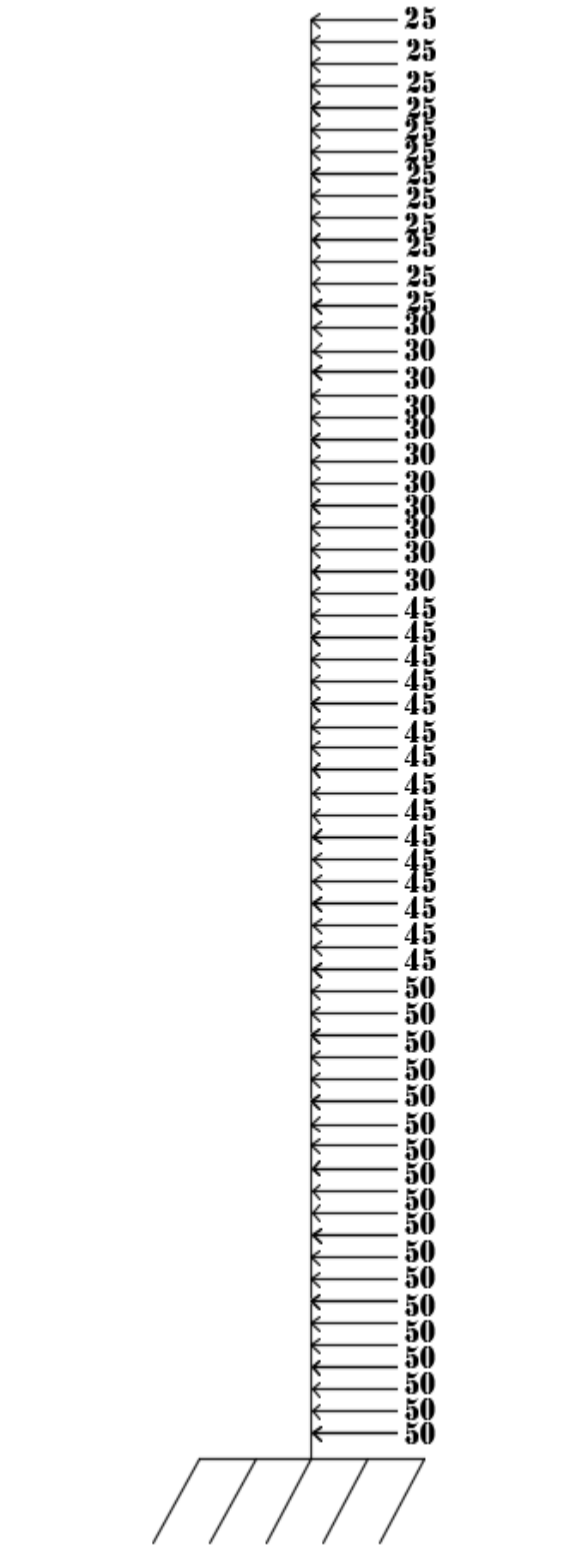

Fig. 3- 5: Shear Force Diagram for I-section wall.

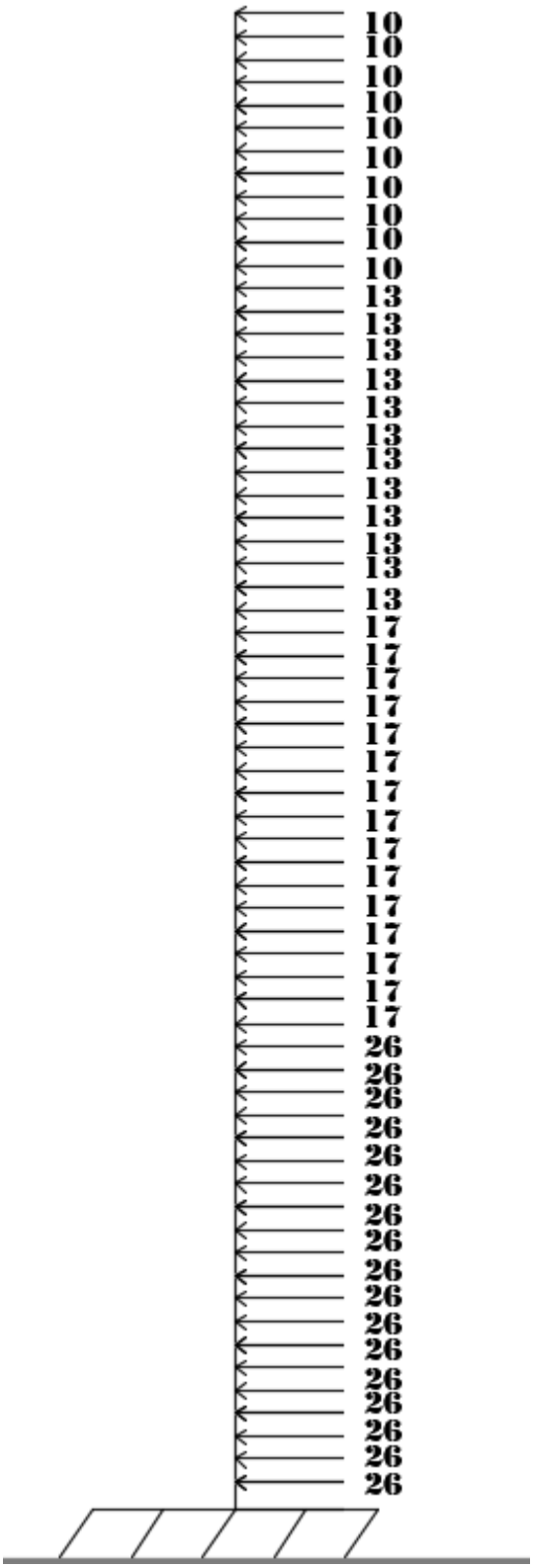

Fig. 3- 6: Shear Force Diagram for Vertical Wall 4200 mm long.

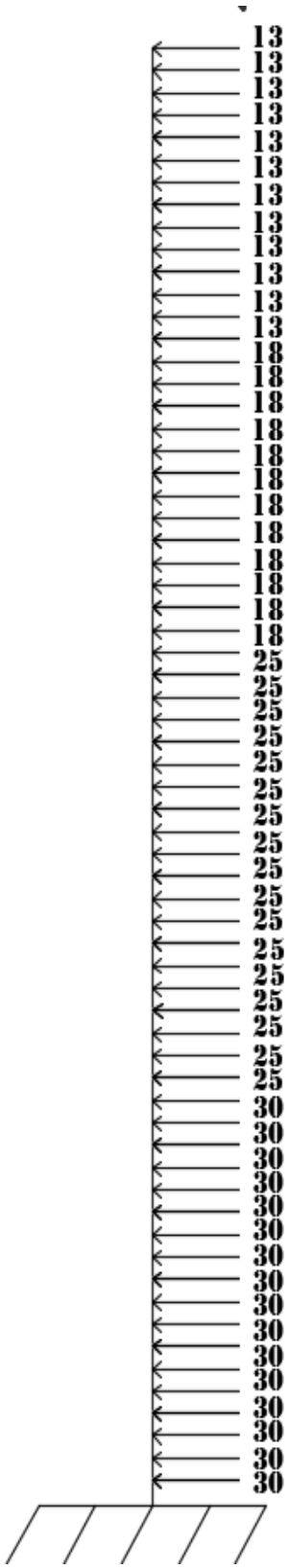

Fig. 3- 7: Shear Force Diagram for L-section wall

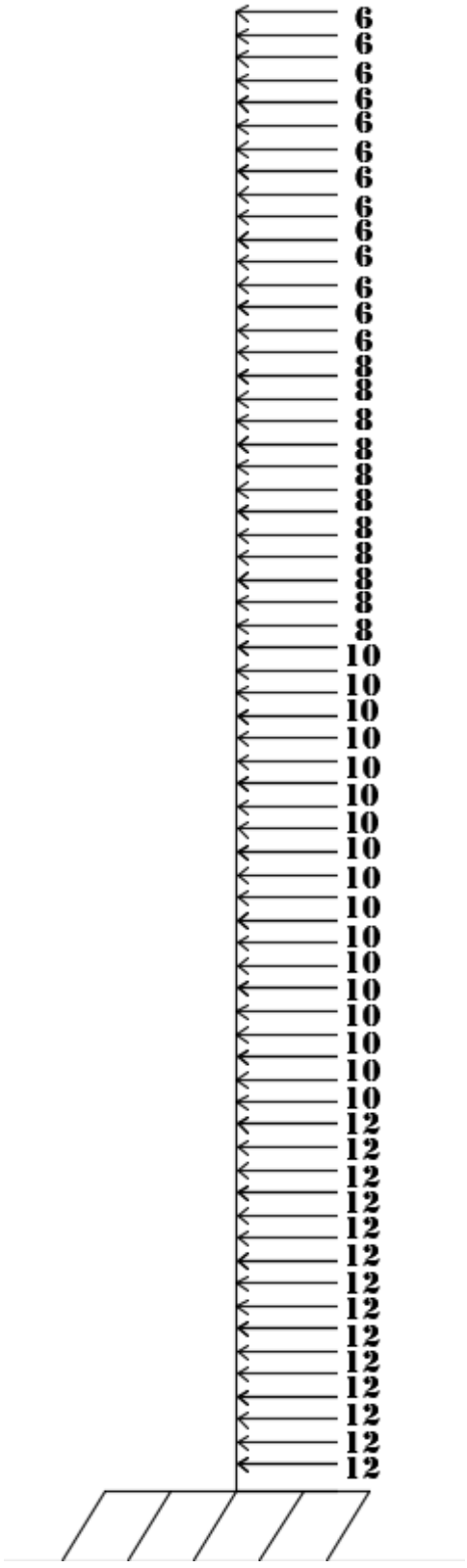

Fig. 3- 8: Shear Force Diagram for inclined section wall

The assumption of equal displacements is often used to assess the plasticity of sections in seismic design. In this study, the same concept is applied here in the case of wind design. In each pushover curve, the linear curve is extrapolated to the value of elastic base shear V_E, resulting from elastic design of the section without taking ductility into account. After getting V_E, the corresponding displacement Δ_{demand} is calculated. Then by getting the value of yield displacement (Δ_{yield}) and getting the ratio $\Delta_{demand}/\Delta_{yield}$, ductility demand can be evaluated.

Fig. 3- 9 Shows the Idealized load – displacement relationship of a frame structure as per FEMA 356 in terms of base shear plotted versus top displacement. In the same figure, an idealized bilinear elastic-perfectly plastic representation of this nonlinear behaviour is shown on the graph. A notable parameter in this figure is ductility demand (μ) which is defined as the ratio of the displacement corresponding to the elastic base shear Δ_{demand}, and the displacement Δ_y corresponding to the global yield base shear (V_y) of the idealized bilinear curve.

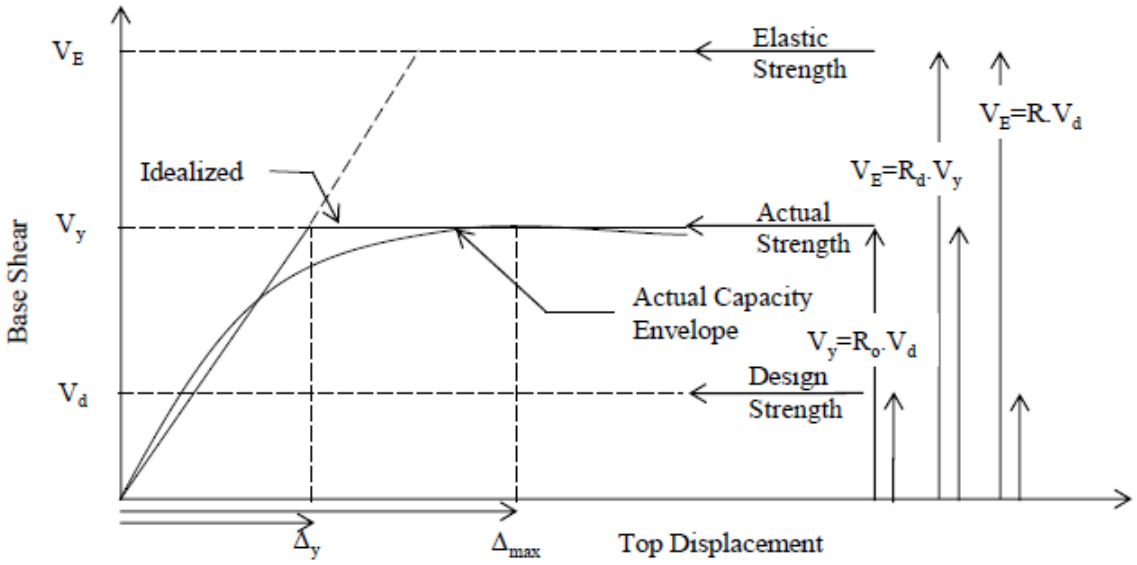

Fig. 3- 9: Idealized Load – Displacement relationship and ductility demand (μ) (Chopra and Goel, 1999)

3.3 Results and discussion:

Non-linear static analysis is done on the reduced shear wall modules marked in the layout in **Fig. 3- 10**. Reduction in shear wall thickness is done based on reduction in wind load resonant component by a factor of R=2, which resulted in reduction in concrete shear wall thicknesses with a factor ranging between 1.15 to 1.25 applied on different shear wall modules. The four shear wall modules in the lateral load resisting system are I-shaped shear wall, Vertical wall 4200 mm long, the inclined shear walls on the two sides of the layout close to the slab edges, and L-shaped shear walls.

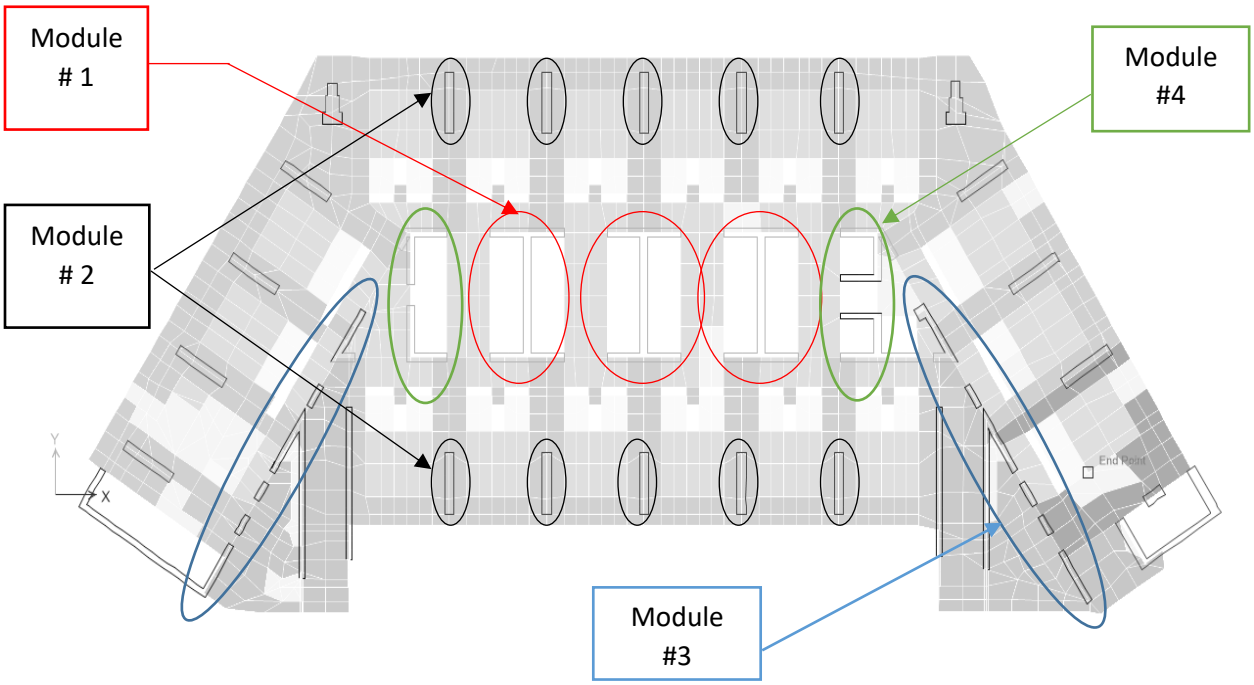

Fig. 3- 10: Structural Layout showing governing shear walls in Lateral Load Resisting System (ETABS FE Model)

For each shear module, proper detailing is provided as per NBCC 2010 to ensure the section possesses enough ductility. NBCC 2010 categorized reinforced concrete sections into three categories based on level of ductility provided which the designer can control through abiding by certain reinforcement provisions: high, moderate and limited ductility. In this study, shear wall sections are reinforced to ensure high ductility, which was used as a baseline for comparison with other ductility levels in terms of assessing inelastic behaviour.

3.3.1 Module #1: I-Section Pushover analysis results:

First shear wall module that is tested for non-linear static pushover analysis is the I-Section shaped shear wall. Load pattern applied in the analysis is obtained from the shear force diagram of the wall resulting from linear analysis of the building. Level of axial load is an important issue when conducting non-linear analysis. For this shear wall, axial force P is found to be 83743 kN. **Fig. 3-11** shows the pushover curve for this shear wall module.

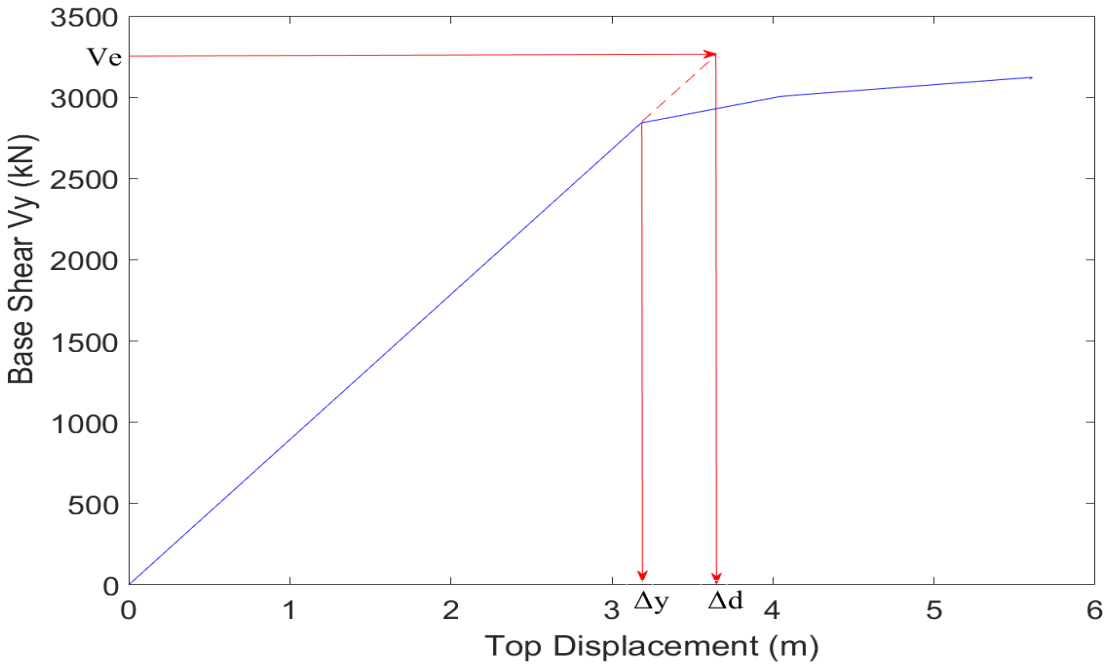

Fig. 3- 11: Pushover Load – Displacement Curve for I-Section shear Wall

Load combination used for evaluating the level of axial force is 1.25 Dead Load + 0.5 Live Load as this is the combination used in wind design as per NBCC 2010.

Adopting the concept of equal displacements, displacement corresponding to the elastic base shear on the pushover curve is divided by the yield displacement and ductility demand μ is found to be 1.17.

Plastic moment M3 is plotted against the plastic hinge rotation as shown in **Fig. 3- 12**. On the same graph also, the backbone curve of the member is plotted to show the acceptance criteria defined by ASCE/SEI 41-13.

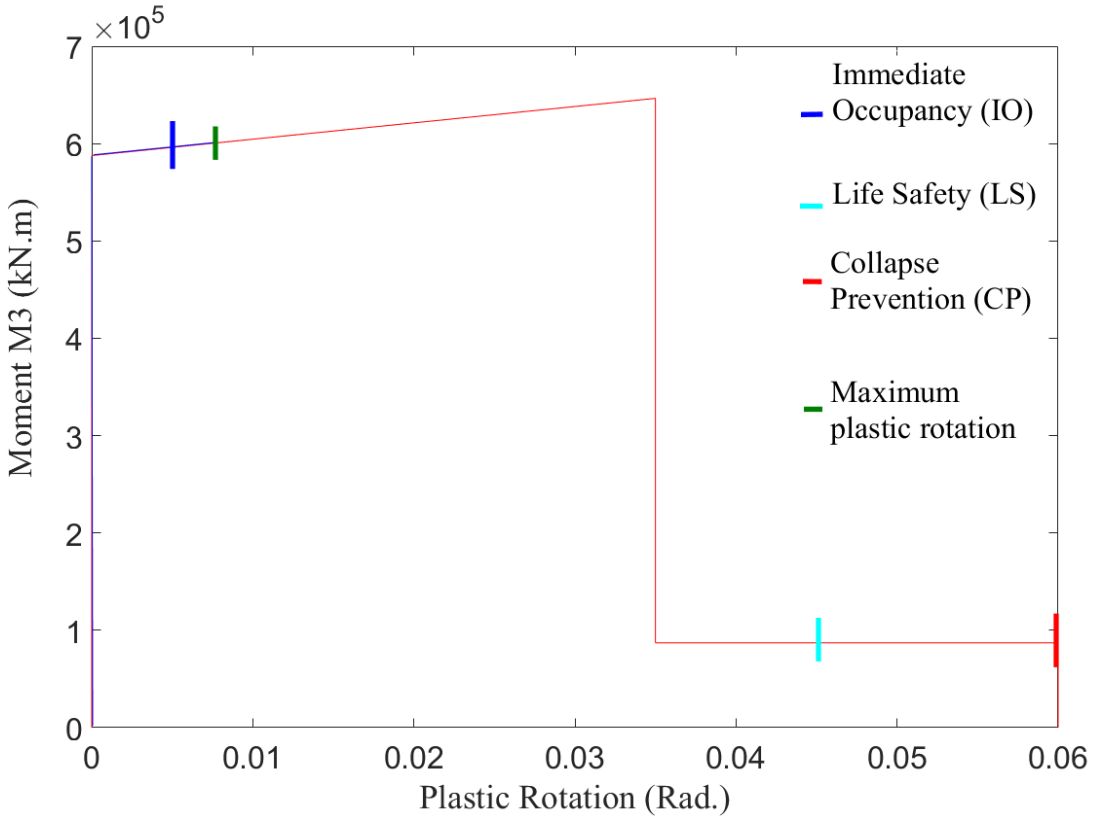

Fig. 3- 12: Moment – Rotation Curve for I-Section shear wall

It can be observed from **Fig. 3-12** that the maximum plastic rotation experienced by the member is 0.008 rad. Which is very close to immediate occupancy (IO) limit which is 0.005 rad.

3.3.2 Module #2: Vertical Wall 4200 mm long Module Pushover analysis results:

The Second Shear wall module in which static pushover curve is carried out is the Verical wall 4200 mm long. Value of axial load P from the full model was 49860 kN. Assuming equal displacements theory, the value of displacements corresponding to elastic base shear V_e divided by the yield displacements gives the ductility demand of the section which is found to be 1.3. **Fig. 3- 13** shows the pushover curve for this shear wall module.

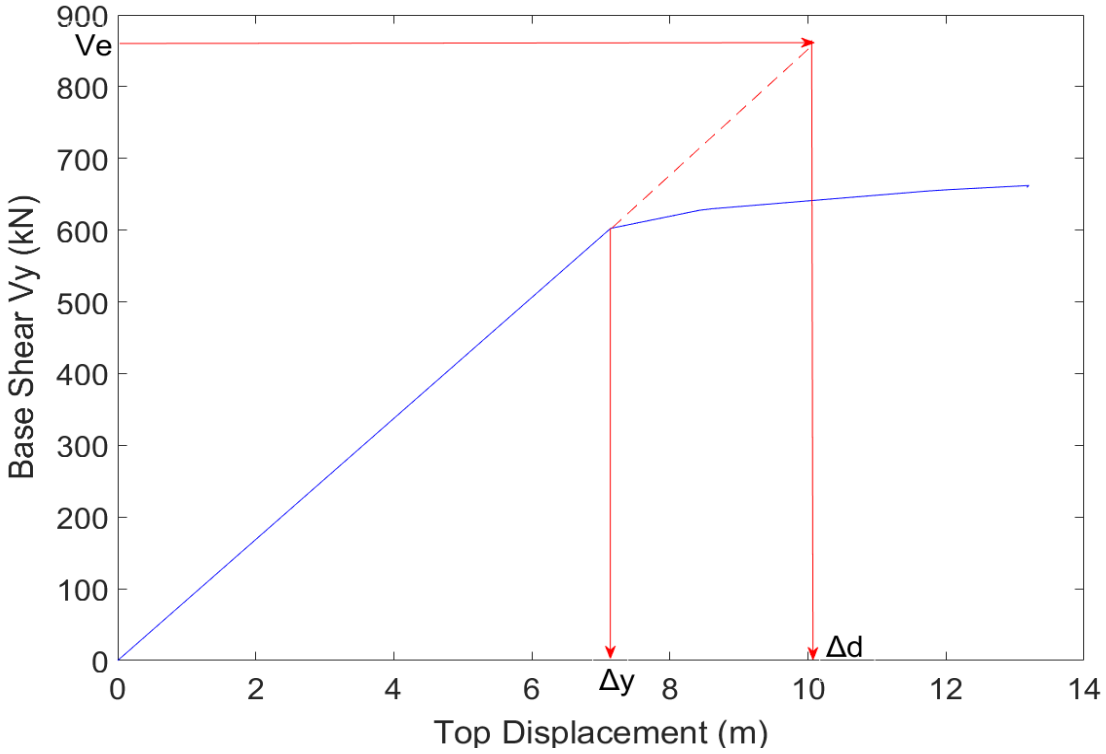

Fig. 3- 13: Pushover Load – Displacement Curve for vertical section shear Wall

Adopting the concept of equal displacements, displacement corresponding to the elastic base shear on the pushover curve is divided by the yield displacement and ductility demand μ is found to be 1.3.

Plastic moment M3 is plotted against the plastic hinge rotation as shown in **Fig. 3- 14** . On the same graph also, the backbone curve of the member is plotted to show the acceptance criteria defined by ASCE/SEI 41-13.

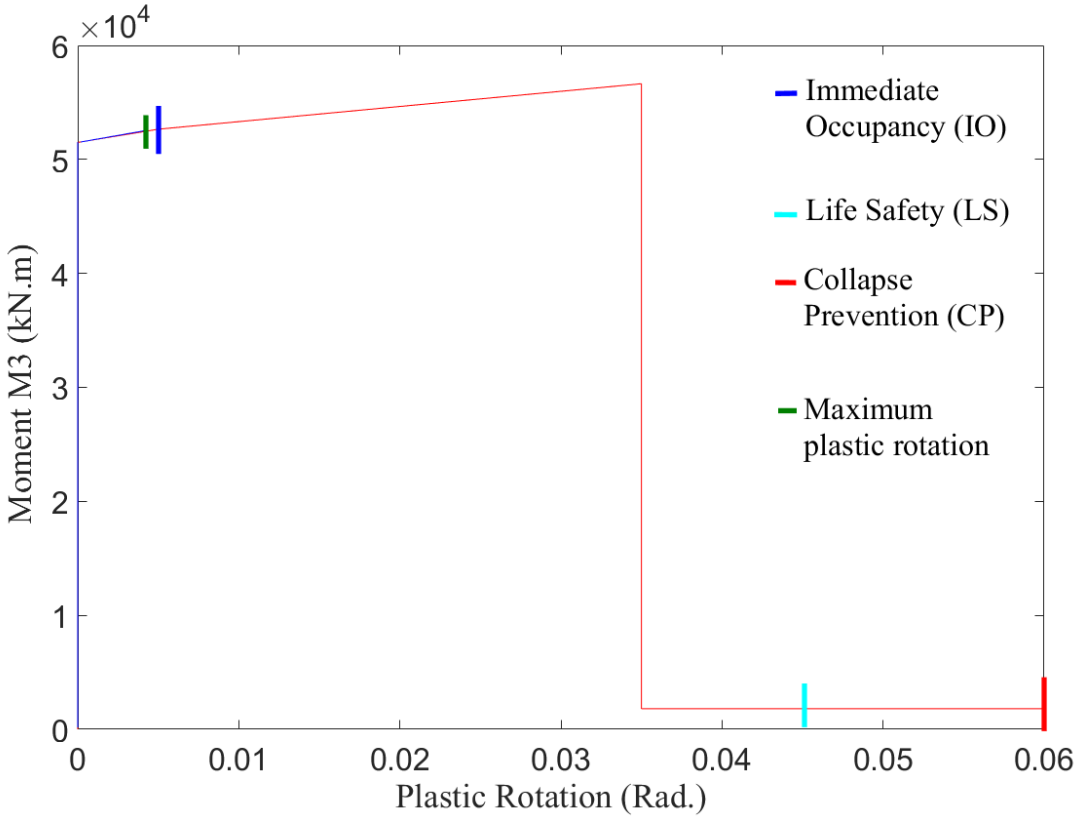

Fig. 3- 14: Moment – Rotation Curve for vertical section shear wall

It can be observed from **Fig. 3- 14** that the maximum plastic rotation experienced by the member is 0.004 rad. Which is very close to immediate occupancy (IO) limit which is 0.005 rad.

3.3.3 Module #3: L-Section Module Pushover analysis results:

The third module of shear walls that is evaluated under static pushover analysis is the L-section shaped shear wall. Axial load P applied on this section is 51225 kN. Assuming equal displacements, ductility demand is calculated by dividing Δ_{demand} / $\Delta_{yield.}$ This value is found to be 1.25. **Fig. 3- 15** shows the pushover curve for this shear wall module.

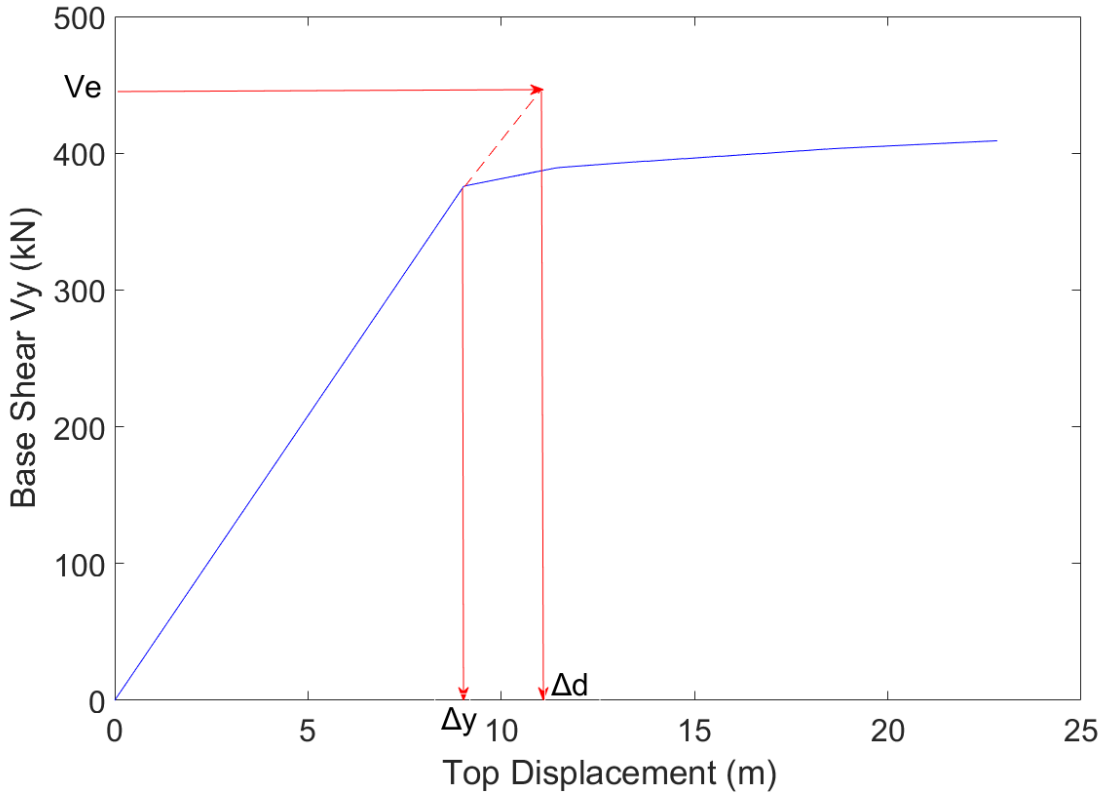

Fig. 3- 15: Pushover Load – Displacement Curve for L-section shear Wall

Plastic moment M3 is plotted against the plastic hinge rotation as shown in **Fig. 3- 16**. On the same graph also, the backbone curve of the member is plotted to show the acceptance criteria defined by ASCE/SEI 41-13.

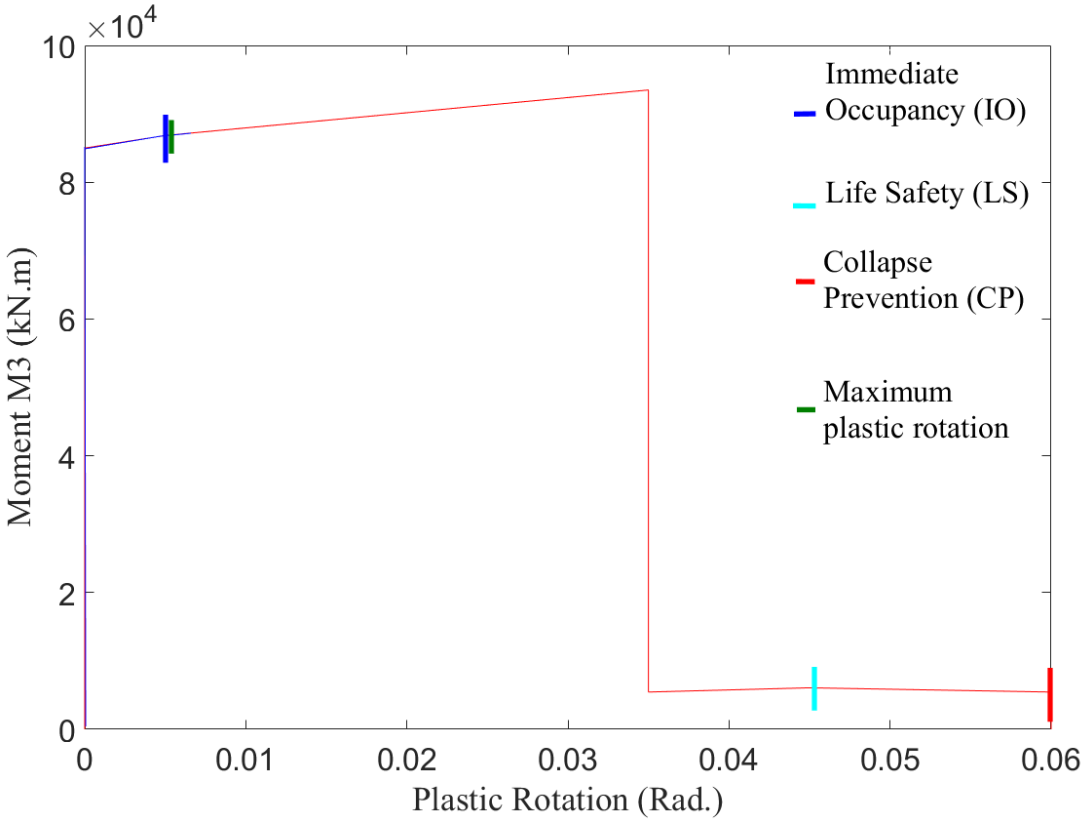

Fig. 3- 16: Moment – Rotation Curve for L- section shear wall

It can be observed from **Fig. 3- 16** that the maximum plastic rotation experienced by the member is 0.0053 rad, which is very close to immediate occupancy (IO) limit which is 0.005 rad.

3.3.4 Module #4: Inclined Wall Module Pushover analysis results:

The fourth module of shear walls that is evaluated under static pushover analysis is the L-section shaped shear wall. Axial load P applied on this section is 51225 kN. Assuming equal displacements, ductility demand is calculated by dividing Δ_{demand} / $\Delta_{yield.}$ This value is found to be 1.2. **Fig. 3- 17** shows the pushover curve for the inclined shear wall module.

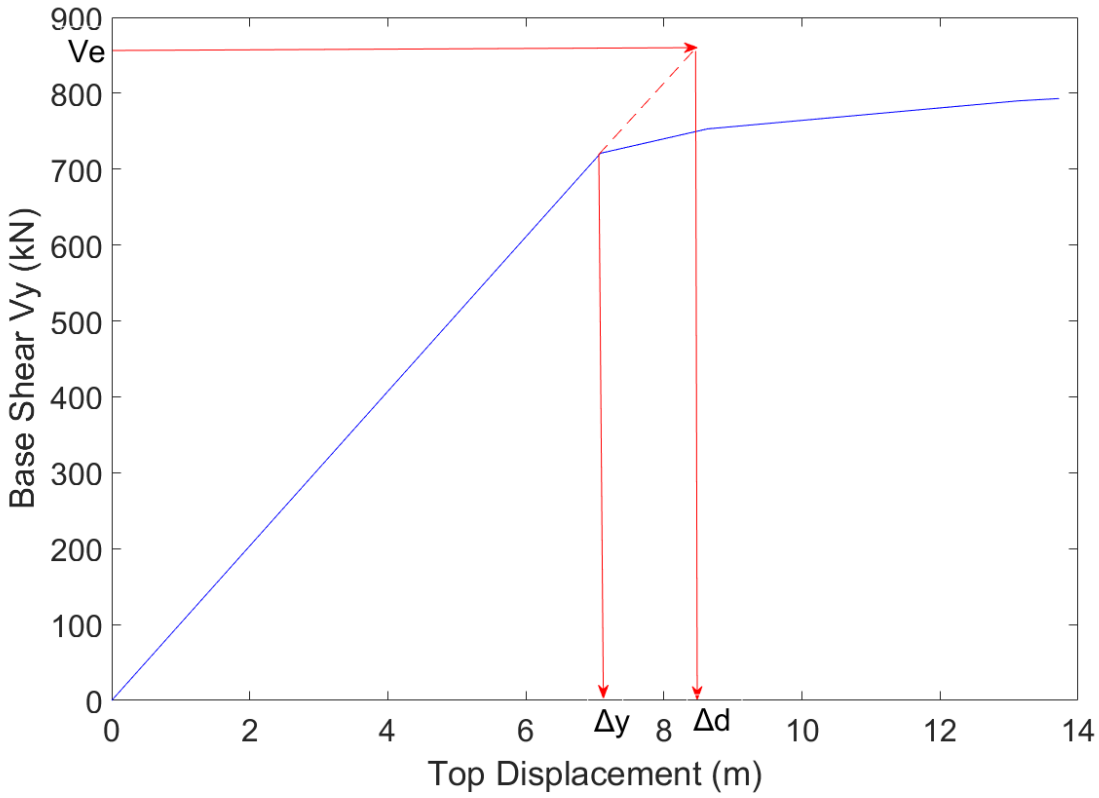

Fig. 3- 17: Pushover Load – Displacement Curve for Inclined shear Wall

Plastic moment M3 is plotted against the plastic hinge rotation as shown in **Fig. 3- 18**. On the same graph also, the backbone curve of the member is plotted to show the acceptance criteria defined by ASCE/SEI 41-13.

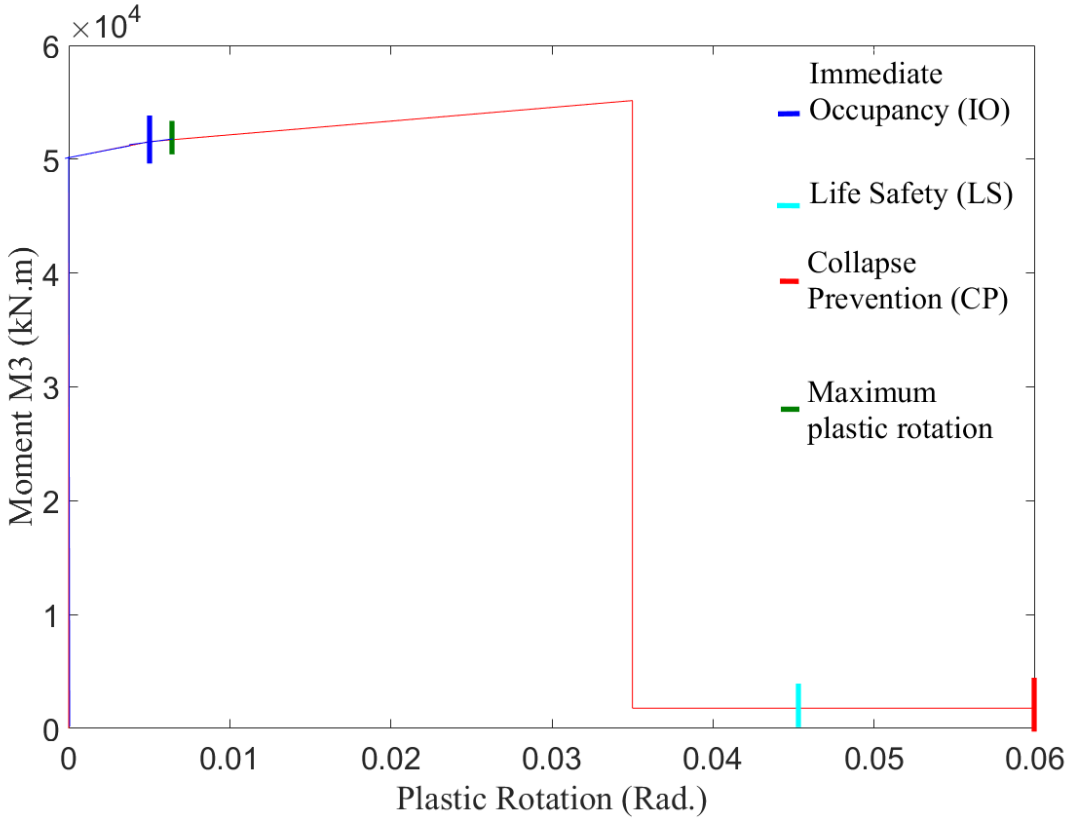

Fig. 3- 18: Moment – Rotation Curve for Inclined shear wall

Table 3- 3 shows a comparison between ductility demand values μ for different shear wall modules.

Table 3- 3: Ductility demand values for different shear wall modules

Shear Wall Module	Ductility Demand (μ)
I - Section	1.17
Vertical Wall (4200 mm long)	1.3
L – Section	1.25
Inclined shear walls	1.2

Table 3- 4 shows a comparison between target performance level reached for each wall cross section.

Table 3- 4: Target performance reached for different shear wall modules

Shear Wall Module	Ductility Demand (μ)
I - Section	Between IO and LS
Vertical Wall (4200 mm long)	Smaller than IO
L – Section	Between IO and LS
Inclined shear walls	Between IO and LS

3.4 Effect of ductility of Shear walls on Non-linear behaviour and Performance Criteria:

In this section, a parametric study is presented, by changing the level of ductility of all reduced shear walls, and monitoring the plastic deformations. Furthermore, inelastic rotations are compared with performance limits defined by ASCE/SEI 41-13 in table 10-8. The Designer always

selects the level of ductility in all reinforced concrete members depending on the desired locations of plastic hinge formation and failure or collapse mechanisms.

In this study, the level of ductility of reinforced concrete shear walls is changed from ductile to moderate ductile. This is achieved by changing the reinforcement details of the shear wall, and abiding by moderate ductility code provisions defined by NBCC 2010.

3.4.1 I-Section Moment Rotation curve and Acceptance Criteria with Moderate Ductility

Pushover analysis is conducted again on the same I-Section but this time given different reinforcement detailing and shear reinforcement ratio, which corresponds to different level of ductility. **Fig. 3- 19** shows the moment rotation curve and hinge response in the I-section shear wall in case it's designed as moderately ductile.

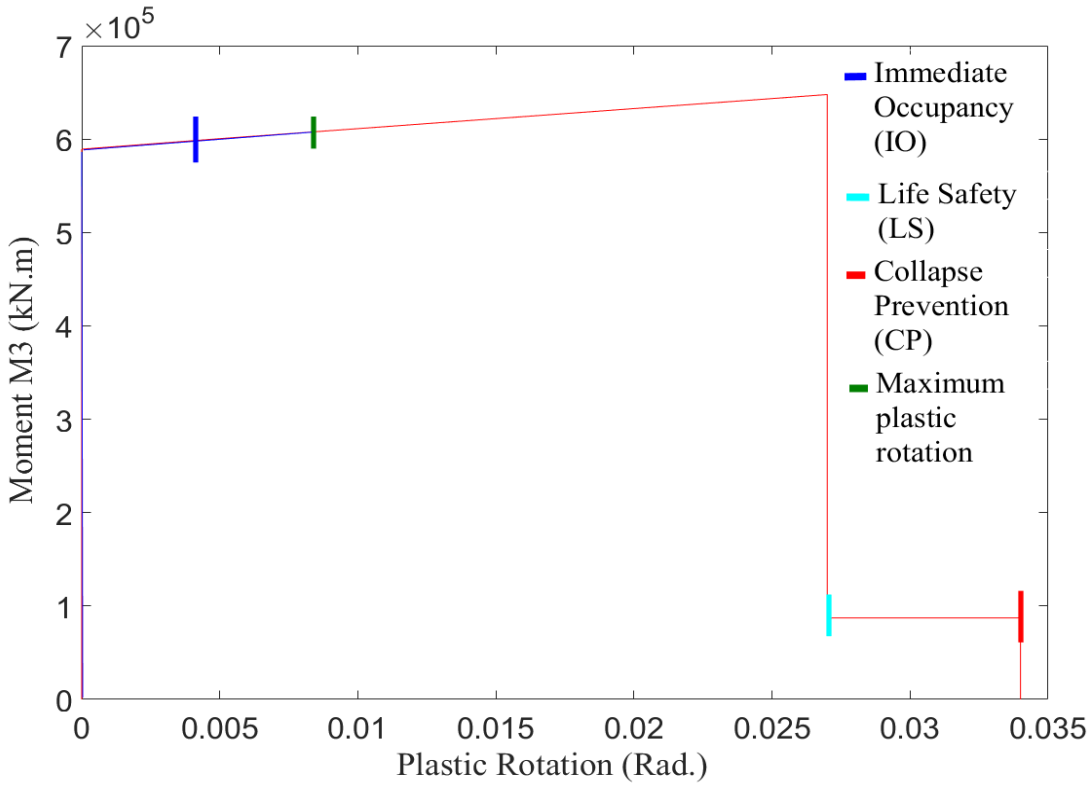

Fig. 3- 19: Moment – Rotation Curve for I-Section shear wall with moderate ductility

It can be observed from the figure that the section is still between Imeediate Occupancy (IO) (0.005 rad.) and Life Safety (0.027) limits with a maximum plastic rotation of 0.008 rad.

3.4.2 Vertical Wall 4200 mm Moment Rotation curve and Acceptance Criteria with Moderate Ductility

The vertical wall 4200 mm long is analyzed again providing different detailing and different ductility level (moderate ductility). Hinge response shown in **Fig. 3- 20** indicates that the plastic hinge is still before the Immediate occupancy limit (0.005 rad.) with a value of plastic rotation of 0.004 rad.

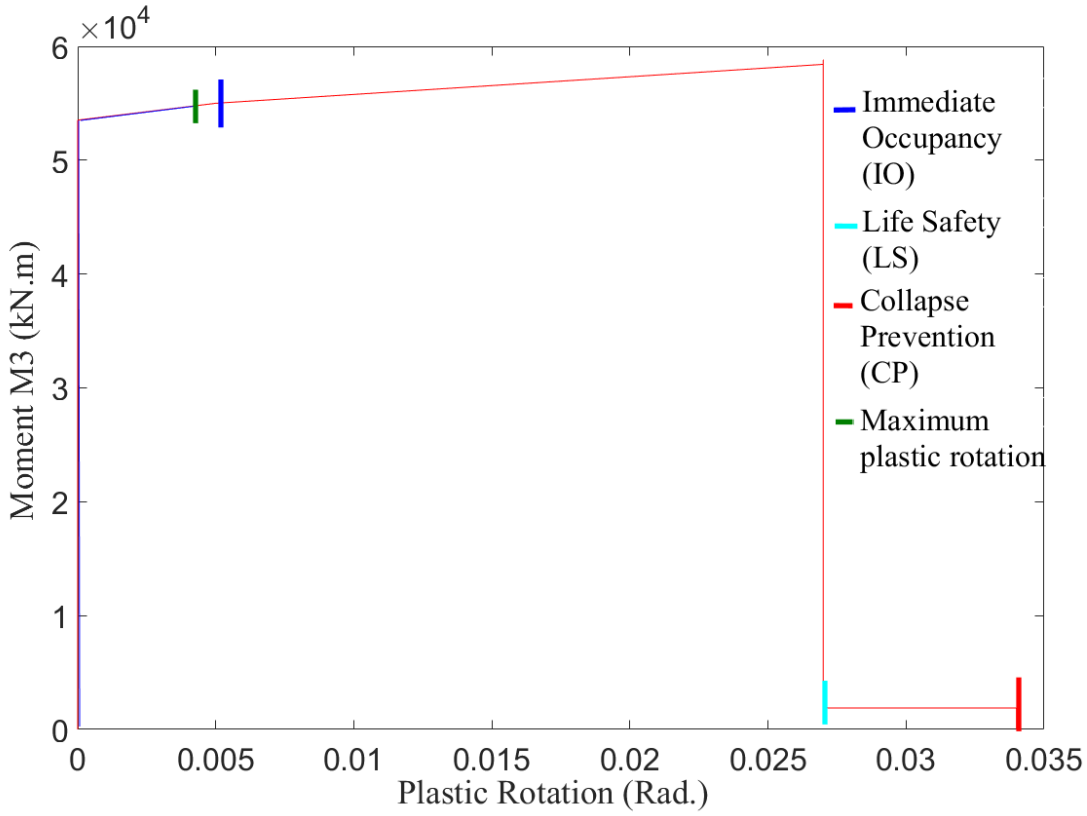

Fig. 3- 20: Moment – Rotation Curve for Vertical shear wall 4200 mm with moderate ductility

3.4.2 I-Section Moment Rotation curve and Acceptance Criteria with Limited Ductility

Pushover analysis is conducted again on the same I-Section but this time given different reinforcement detailing and shear reinforcement ratio, which corresponds to different level of ductility (limited ductility)**. Fig. 3- 21** shows the moment rotation curve and hinge response in the I-section shear wall in case it is designed as limited ductile.

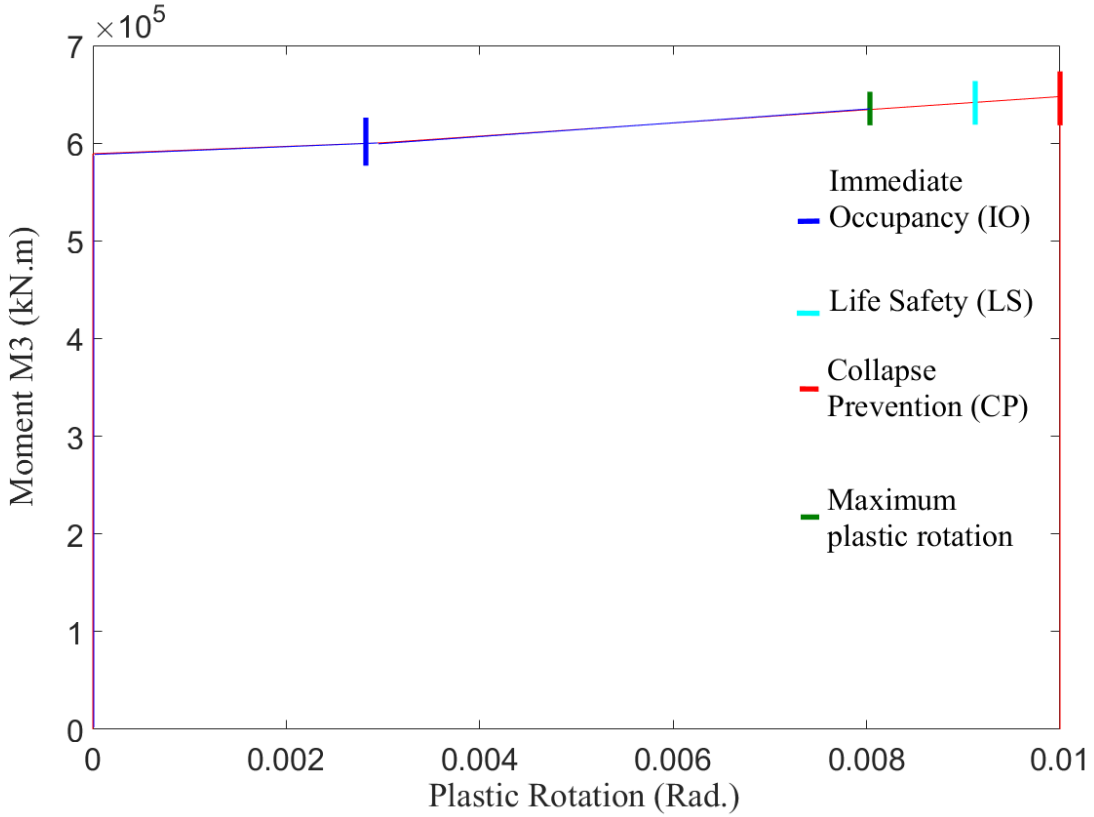

Fig. 3- 21: Moment – Rotation Curve for I-shear wall 4200 mm with limited ductility

It can be observed from the **Fig. 3- 21** that the section is still between Immediate Occupancy (IO) (0.003 rad.) and Life Safety (0.009) limits with a maximum plastic rotation of 0.008 rad.

3.4.3 Vertical wall 4200 mm Moment-Rotation curve and Acceptance Criteria with Limited Ductility

Pushover analysis is conducted again on the same vertical section but this time given different reinforcement detailing and shear reinforcement ratio, which corresponds to different level of ductility (limited ductility). **Fig. 3- 22** shows the moment rotation curve and hinge response in the vertical section shear wall in case it is designed as limited ductile.

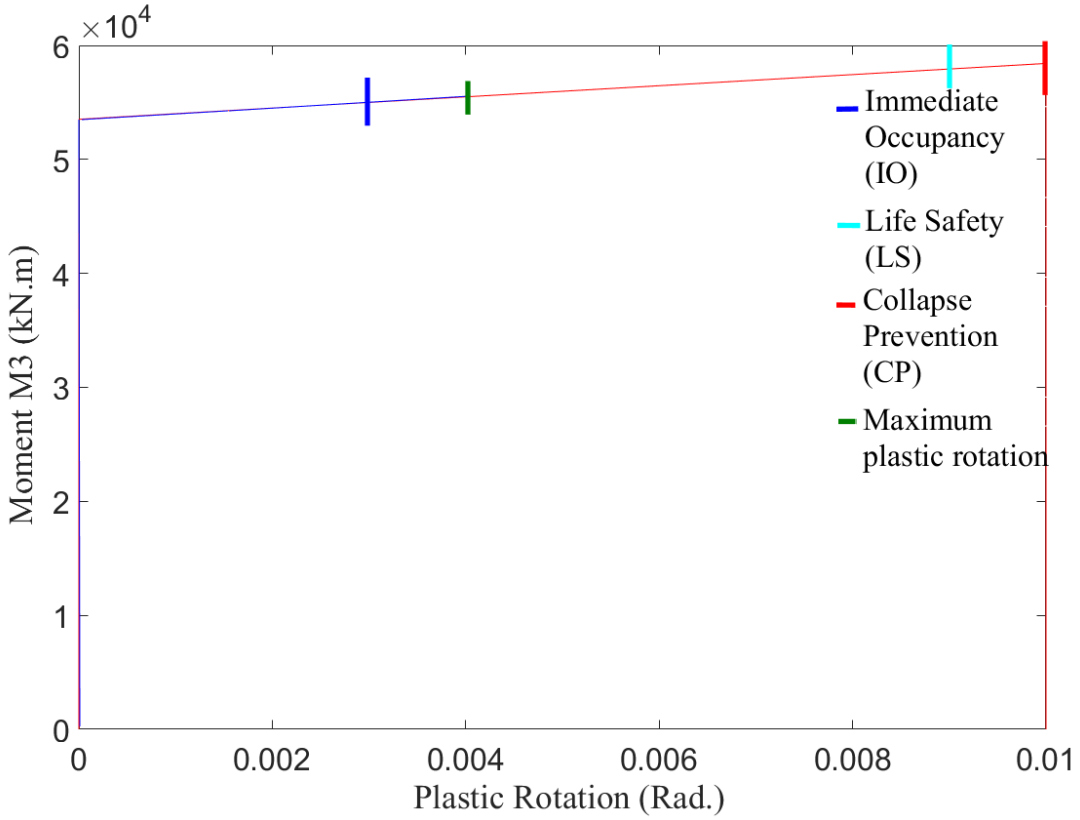

Fig. 3- 22: Moment – Rotation Curve for Vertical shear wall 4200 mm with limited ductility

It can be observed from the **Fig. 3- 22** that the section is still between Immediate Occupancy (IO) (0.003 rad.) and Life Safety (0.009) limits with a maximum plastic rotation of 0.004 rad.

CHAPTER 4

SUMMARY AND CONCLUSIONS

4.1 Summary

The research conducted in this thesis investigates the application of the ductility-based approach employed in seismic design, on high-rise buildings subjected to extreme wind loads. In addition to that, inelastic actions experienced by concrete shear walls are evaluated in terms of ductility demand (μ), and target performance levels reached for different ductility levels of shear walls are compared with limits of acceptance criteria defined by current codes (ASCE/SEI 41-13). First, a 3D numerical finite element model is developed for an existing 65-storey building tested previously in the Boundary Layer Wind Tunnel (BLWT) facility in the University of Western Ontario. The building lateral load resisting system is concrete shear walls. Second, dynamic time history analysis is conducted to evaluate building total responses. This is followed by conducting Quasi-static analysis to evaluate Mean + Background responses to separate the total response into Mean, Background and Resonant component. A load reduction factor "R" is implemented on wind resonant component, and a new set of loads are applied, and shear wall cross-sections are redesigned accordingly. Third, a comparison between building dynamic characteristics and total responses before and after reducing shear wall cross-sections is presented. Furthermore, non-linear finite element models were developed for individual shear walls to conduct static pushover analysis. Ductility demand (μ) is calculated for each shear wall module. Target performance levels reached for each shear wall module are compared with limits of acceptance criteria defined by ASCE/SEI 41-13. Furthermore, analysis is repeated for different ductility levels of shear walls.

4.2 Conclusions:

A high-rise 65-story building subjected to wind loads was considered in this study to assess ductility-based design approach for high-rise buildings under extreme wind loads. Pressure coefficient (C_P) time history values were taken from wind tunnel test and used to evaluate wind story forces. A 3D model was constructed for the building and time-history dynamic analysis was conducted to evaluate total wind responses of the structure. Quasi-static analysis was conducted to capture the mean + background components of the response (V_Q (t)) and separate them from the resonant part (V_R (t)). Resonant part of the response was reduced by a factor "R" and shear walls were redesigned under reduced load to assess structure's dynamic characteristics. The case study results presented in this chapter shows that by reducing wind resonant component by a factor of "2", and redesigning wind load resisting system members under reduced loads results in reduction in concrete walls dimensions by 20-25% with no major change in the fundamental period. Fundamental period of the period increased by 6% only. Peak responses did not increase when making the building more flexible, with a decrease of 7%. A parametric study was done on the "R" reduction factor studying its effect on building response. It was found that as a result of increasing R factor, the peak base shear decreases, and the fundamental period of the building increases but the variation doesn't exceed 6%.

In the second part of the study, non-linear static pushover analysis is done on several shear wall modules, which were reduced in thickness by a percentage ranging between 20 % – 25 %, depending on the reduction procedure presented in chapter 2. Results of wind responses and initial strength design of shear walls were taken from a full finite element model of a high-rise 65-storey building.

A reduction factor R = 2 was selected by the designer and applied on wind resonant component of the response, and a certain level of ductility has to be achieved. The study presented in this chapter elaborates the inelastic behaviour for different sections of reinforced concrete shear walls, and assesses the ductility demand in these sections to justify the application of this reduction factor.

Plastic rotations experienced by plastic hinges in shear walls are monitored and compared with Performance Limits defined in current codes (ASCE/SEI 41-13 and FEMA 356). Based on this comparison, the assessment is done on each individual wall and it was checked whether this ductility level and performance is acceptable as the philosophy adopted in seismic design, where controlled inelastic actions are permitted without major loss in strength and the members still have some margin before collapse. Each Performance level or plastic hinge state has to be associated with an action to be taken on the members experiencing inelastic actions as adopted in current building codes. In this study, all members are found to be in the Immediate Occupancy (IO) level, which as per (ASCE/SEI 41-13) is the state where the building is still safe to be occupied immediately after the extreme event occurred during the lifetime of the building.

Furthermore, shear wall sections are evaluated with different levels of ductility. Moderately ductile and limited ductile shear walls are analyzed and it is found that the inelastic behaviour in this case is the same in terms of target performance level reached. Members are still within the Immediate Occupancy (IO) limit. Therefore, this study concludes that members that are susceptible to excessive inelastic actions due to wind can still be detailed as limited ductile as per current building codes (NBCC 2010) which will most likely be the case for buildings governed by wind loads.

The following conclusions are obtained from application of a ductility-based approach for a high-rise building subjected to extreme wind loads:

1- Concrete shear wall cross sections were reduced by 20-25% as a result of applying a load reduction factor to wind resonant component by R =2.
2- Fundamental period of the structure changed by only 6% after reducing shear wall cross-sections.
3- Total base shear of the building in the two orthogonal directions did not increase as a result of reducing shear wall cross-sections, and almost remained the same.
4- The same reduction procedure was repeated with R = 3, with no major change in fundamental period and building responses for the studied building.

The conclusions drawn from conducting static pushover analysis on reduced cross-sections of concrete shear walls are:

1- Ductility demand values for different shear wall modules, applying the assumption of equal displacements, are evaluated, and values are ranging between 1.17 and 1.3.
2- Target performance levels reached for ductile shear walls are between Immediate Occupancy (IO) and Life Safety (LS).
3- In case of limited ductile shear walls, target performance level reached is still in within the Immediate Occupancy (IO) range.

It should be noted that these conclusions are only limited to this case study and only for concrete shear walls Further research needs to be conducted in a probabilistic manner in order to reach a more general conclusion.

4.3 Recommendations for future work:

The current study investigated the application of ductility-based approach on high-rise building subjected to extreme wind loads, and assessed the inelastic actions experienced by concrete shear walls. The following investigations are suggested for future research:

1- Conducting non-linear static pushover analysis for the full model of the building using a powerful finite element tool, to monitor the sequence of plastic hinge formation within different members in the lateral load resisting system.

2- Carrying out dynamic time-history analysis on the reduced cross section of shear walls, to evaluate the hysterias loops, and assess the stiffness degradation due to large number of loading cycles.

3- Trying different number of cycles, and assessing the stiffness degradation in each case.

4- Repeating the analysis for several wind events with different return periods.

5- Extending the study on different lateral load resisting systems as moment resisting frames or frame-wall systems.

REFERENCES

Alan Davenport Wind Engineering GroupG, 2007. “Wind Tunnel Testing: A General Outline.” (May): G2–4.

ACI Committee 318. (1995). Building code requirements for structural concrete: (ACI 31895); and commentary (ACI 318R-95). Farmington Hills, MI: American Concrete Institute.

American Society of Civil Engineers (ASCE). (2010). Minimum Design Loads for Buildings and Other Structures (7-10), Reston, VA.

American Society of Civil Engineers (ASCE). (2013). Seismic Evaluation and Retrofit of Existing Buildings (41-13), Reston, VA.

Augusti, G., and M. Ciampoli. 2008. “Performance-Based Design in Risk Assessment and Reduction.” 23: 496–508.

Bakhshi, A. and Nikhbakht, H. 2011. “Loading Pattern and Spatial Distribution of Dynamic Wind Load and Comparison of Wind and Earthquake Effects along the Height of Tall Buildings.” In Proceedings, 8th International Conference on Structural Dynamics (Eurodyn), July 4-6, Leuven, Belgium.,.

Bashor, R., and A. Kareem. 2007. “Probabilistic Performance Evaluation of Buildings : An Occupant Comfort Perspective.”

Bracci J., Kunnath S., Reinhorn A. Seismic performance and retrofit evaluation of reinforced concrete structures. Journal of Structural Engineering, ASCE 1997; 123(1):3–10.

British Standrads Institute. 1996. Eurocode 8: Design Provisions for Earthquake Resistance of Structures: British Strandards Inistitution.

Canada, National Research Council of. 2010. “National Building Code of Canada.”

Ciampoli, M.. Petrini, F. and Augusti, G. 2011a. “Performance-Based Wind Engineering: Towards a General Procedure.” Structural Safety 33(6): 367–78.

Computers and Structures Inc. 2015. “CSI Analysis Reference Manual.” P. 496.

Fajfar.P, Gaspersic,P. (1996) The N2 method for the seismic damage analysis of RC buildings. Earthquake Engineering and Structural Dynamics 1996; 25:31–46.

FEMA. NEHRP guidelines for the seismic rehabilitation of buildings. FEMA 273, Federal Emergency Management Agency, 1996.

Gani, F., and Legeron, F. (2012). “Relationship between specified ductility and strength demand reduction for single degree-of-freedom systems under extreme wind events.” Journal of Wind Engineering and Industrial Aerodynamics, 109, 31–45.

Griffis, L., Patel, V., Muthukumar, S., and Baldava, S. (2012). “A framework for performance-based wind engineering.” Advances in Hurricane Engineering, 1205-1216.

Hart, G. C., and Jain, A. (2013). “Performance based wind design of tall concrete buildings in the Los Angeles region utilizing structural reliability and nonlinear time history analysis.” Proceedings, 12th Americas Conference on Wind Engineering (12ACWE), June 16-20, Seattle, Washington.

Huang, G., and Chen, X. (2007). “Wind load effects and equivalent static wind loads of tall buildings based on synchronous pressure measurements.” Engineering Structures, 29, 2641-2653.

Huang, F. et al. 2015. “Journal of Wind Engineering Performance-Based Design Optimization of Tall Concrete Framed Structures Subject to Wind Excitations.” 139: 70–81.

Judd, J. P., and Charney, F. A. (2014a). “Seismic performance of buildings designed for wind.” Proceedings, Structures Congress, April 3-5, Boston, Massachusetts.

Judd, J. P., and Charney, F. A. (2014b). “Earthquake risk analysis of structures.” Proceedings, 9th International Conference on Structural Dynamics (Eurodyn), June 30–July 2, Porto, Portugal.

Kareem, A., Spence, S. M. J., and Bernardini, E. (2013). Performance-based design of wind excited tall and slender structures. NatHaz Modeling Laboratory, University of Notre Dame, September, South Bend, Illinois.

Saiidi M, Sozen MA (1981). Simple nonlinear seismic analysis of R/C structures. Journal of the Structural Division, ASCE 1981; 107(ST5):937–51.

Hart, G., and Jain, A. 2014. “Performance-Based Wind Evaluation and Strengthening of Existing Tall Concrete Buildings in the Los Angeles Region : Dampers , Nonlinear Time History Analysis and Structural Reliability.” 1274(October 2013): 1256–74.

Ho, E. Mara T. Edey, R. 2008. “King Abdul Aziz Endowment Hotel Tower Mecca , Saudi Arabia.” (May).

Holmes, J. "Wind Loading of Structures Third Edition".

Judd, P. and Charney, A. 2015. “Inelastic Behavior and Collapse Risk for Buildings Subjected to Wind Loads.” (2012): 2089–2100.

Judd, J.P and Charney, F.A (2012) "Inelastic Behaviour and Collapse Risk for Buildings Subjected to Wind Loads." 2483–96.

Muthukumar, S. et al. 2013. “Performance-Based Evaluation of an Existing Building Subjected to Wind Forces.” : 1217–28.

Van de Lindt, J. and Dao, T. 2009. “Performance-Based Wind Engineering for Wood-Frame Buildings.” Journal of Structural Engineering 9445 (November 2003).

Oldfield, P., and Trabucco, D. 2014. “Roadmap on the Future Research Needs of Tall Buildings.” Council on Tall Buildings and Urban Habitat.

Paulotto, C., and M. Ciampoli. “Some Proposals for a First Step towards a Performance Based Wind Engineering.”

Spence, J, et al. 2015. “A First Step towards a General Methodology for the Performance-Based Design of Wind-Excited Structures.” : 1482–93.

Spence et al. 2014. “Performance-Based Design and Optimization of Uncertain Wind-Excited Dynamic Building Systems.” Engineering Structures 78: 133–44.

APPENDICIES

Appendix A:

Story time history wind forces from integrating pressure coefficients

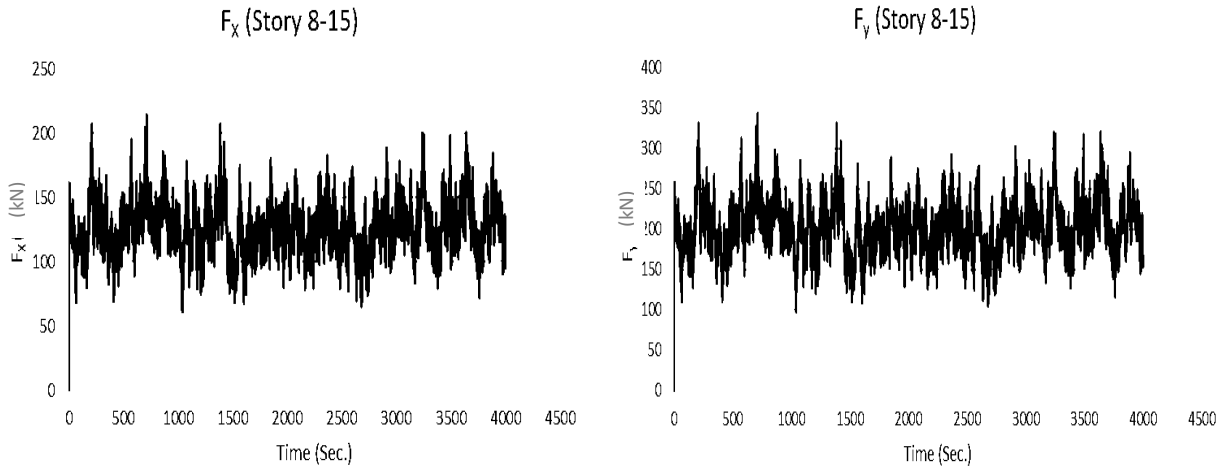

Fig . A-1: Story forces for stories 33-39

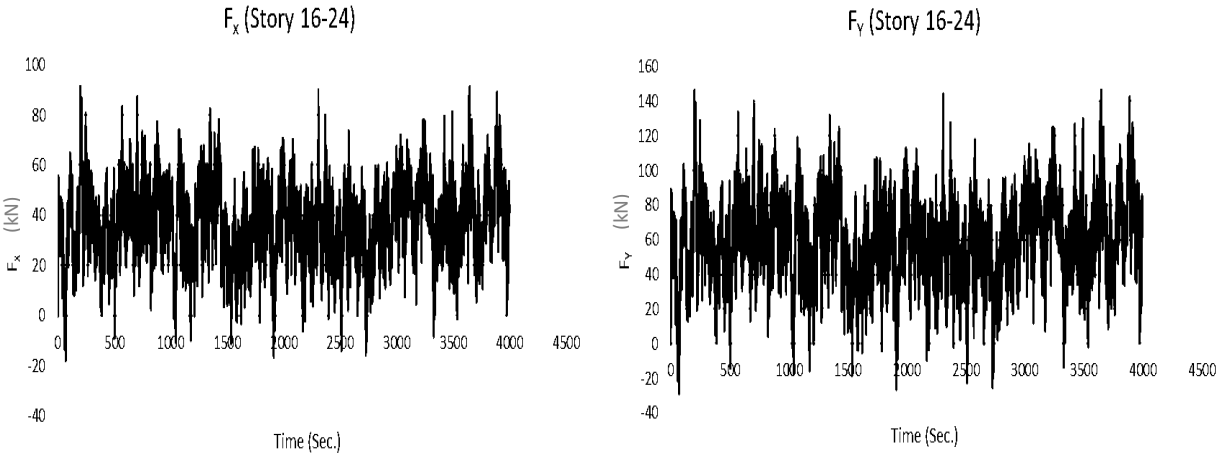

Fig . A-2: Story forces for stories 8-15

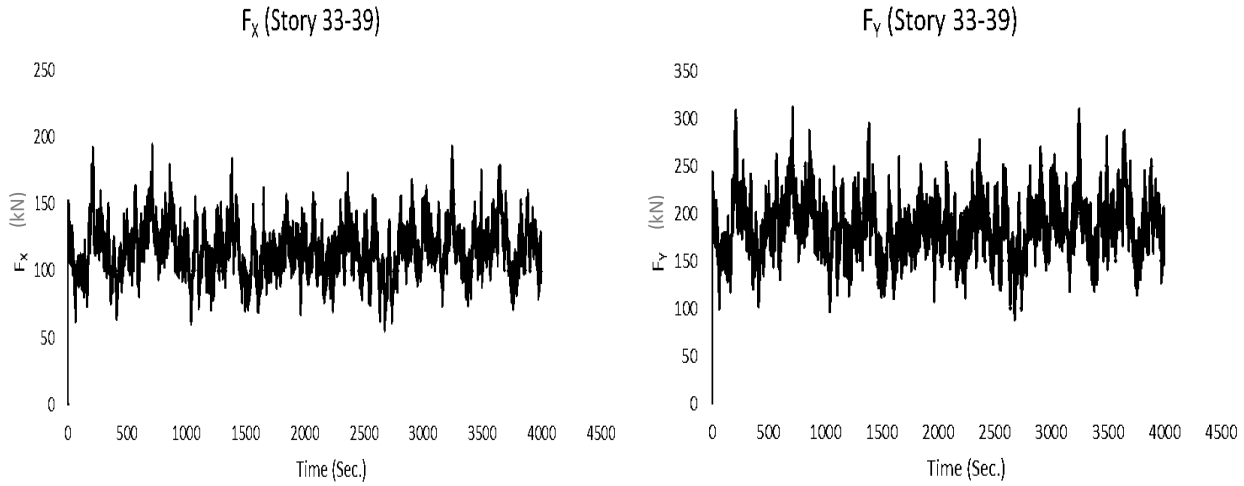

Fig . A-3: Story forces for stories 40-49

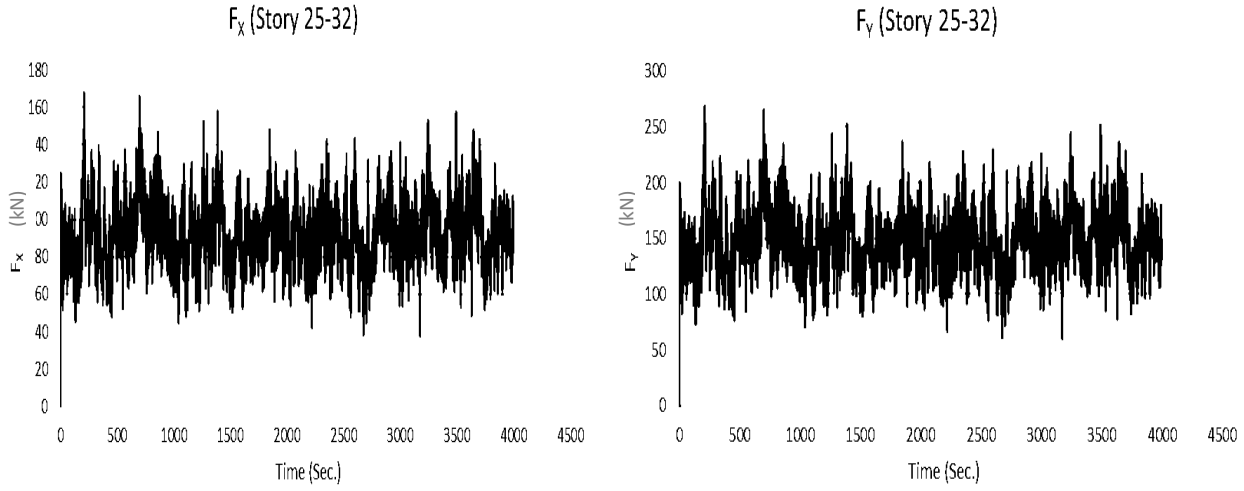

Fig . A-4: Story forces for stories 50-61

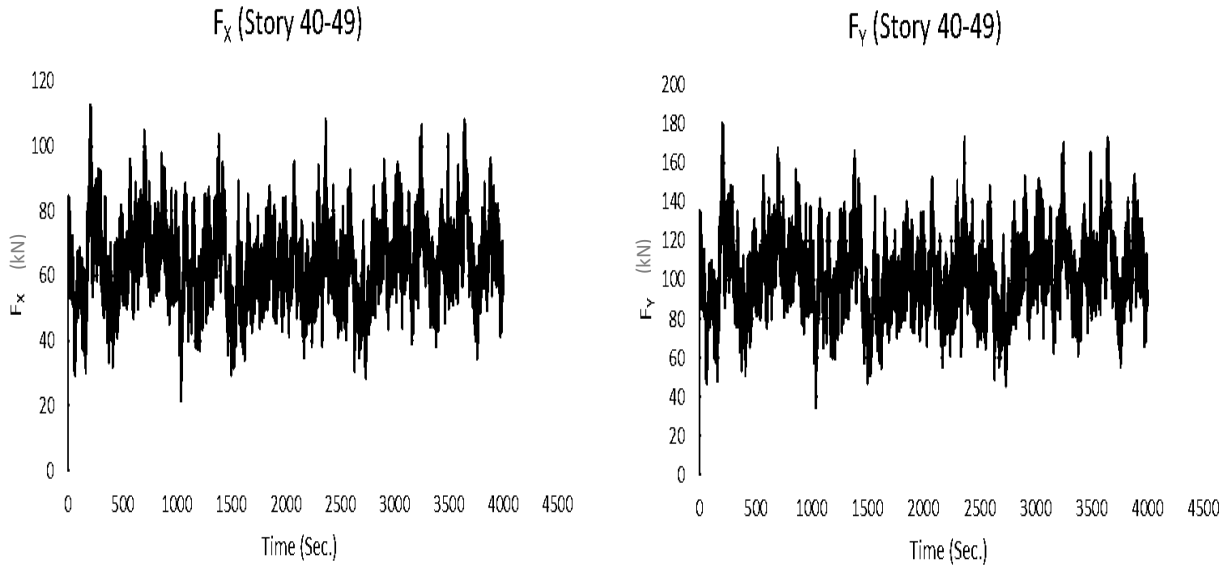

Fig . A-5: Story forces for stories 25-32

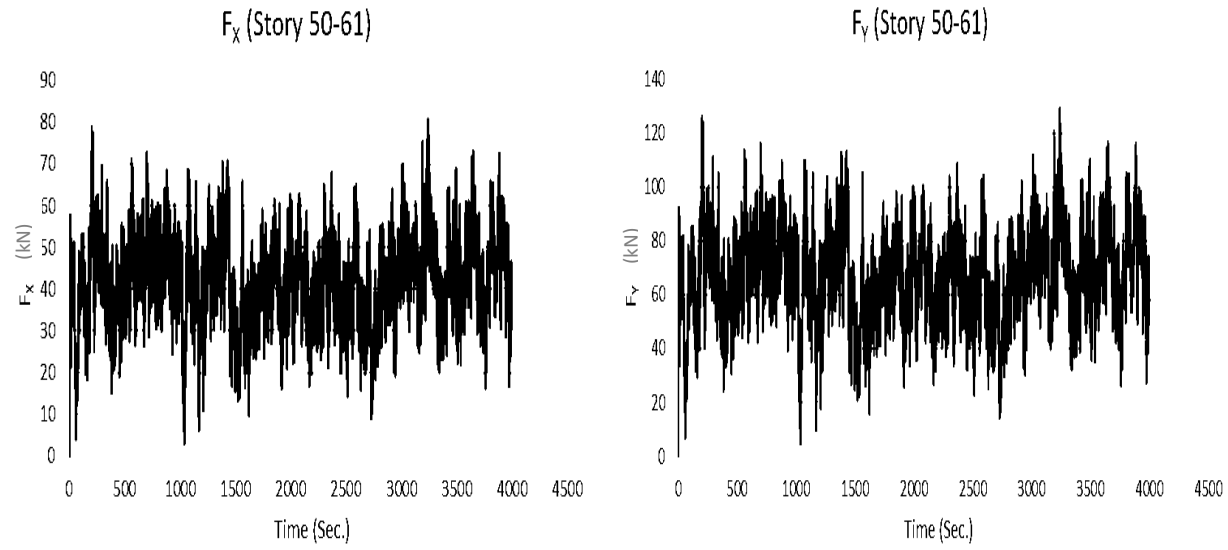

Fig . A-6: Story forces for stories 16-24

Curriculum Vitae

Name:	Fouad Elezaby
Post-secondary Education and Degrees:	Cairo University Giza, Egypt 2008-2013 B.A. The University of Western Ontario London, Ontario, Canada 2015-2017 M.A.
Honours and Awards:	Nominated for the best Teaching Assistant award 2016
Related Work Experience	Teaching Assistant The University of Western Ontario 2015-2017

Publications:

Elezaby F., El Damatty A. “Preliminary Investigation to assess the application of Ductility-Based approach on high-rise Buildings subjected to extreme Wind Loads” The 2017 European-African Conference on Wind Engineering (EACWE) Liege, Belgium, 2017.